DESIGN OF A PRINTED CIRCUIT BOARD FOR A SENSORLESS THREE-PHASE

BRUSHLESS DC MOTOR CONTROL SYSTEM

A Thesis

presented to

the Faculty of California Polytechnic State University,

San Luis Obispo

In Partial Fulfillment

of the Requirements for the Degree

Master of Science in Industrial Engineering

by

Joshua Castle

June 2020

COMMITTEE MEMBERSHIP

TITLE: Design of a Printed Circuit Board for a Sensorless

                             Three-Phase Brushless DC Motor Control System

AUTHOR: Joshua Castle

DATE SUBMITTED: June 2020

COMMITTEE CHAIR: Jianbiao Pan, Ph.D.

                             Professor of Industrial and Manufacturing Engineering

COMMITTEE MEMBER: John Ridgely, Ph.D.

                             Professor of Mechanical Engineering

COMMITTEE MEMBER: Siyuan Xing, Ph.D.

                             Assistant Professor of Mechanical Engineering

ABSTRACT

Design of a Printed Circuit Board for a Sensorless Three-Phase Brushless DC Motor Control

System

Joshua Castle

The use of brushless motors has increased in recent years due to superior performance

characteristics compared with alternatives. The operation of a brushless motor is dependent

upon a separate controller which is often in the form of a printed circuit board. As such, the

size and performance capability of the controller can restrict the performance of the overall

motor control system so advancements of these controllers further the potential use of BLDC

motors. This project outlines the design of a PCB based, sensorless motor controller for

operation of a three-phase BLDC motor powered by a 24 V, high current external supply.

Components used were selected to withstand an ambient temperature environment of 125

degrees C.

The design for this PCB based motor control system was completed but fabrication and

testing of the system was prevented by COVID-19 related restrictions that prohibited the use

of necessary facilities and equipment. The detailed design including component selection,

board layout, and software development is included in addition to a plan for fabrication and

fundamental functional testing. Although no results are available for analysis to bring about

any conclusions, a variety of design strategies and corresponding learnings hold the potential

to be a source of valuable reference to the further study and development of future designs.

Keywords: Brushless DC Motor, Motor Controller, PCB, Sensorless Feedback, Automotive

ACKNOWLEDGMENTS

TABLE OF CONTENTS

LIST OF TABLES

LIST OF FIGURES

LIST OF ABBREVIATIONS

DC   Direct Current

BLDC   Brushless DC

EMF   Electromotive Force

ESC   Electronic Speed Controller

MOSFET   Metal Oxide Semiconductor Field Effect Transistor

DSP   Digital Signal Processing

PCB   Printed Circuit Board

IC   Integrated Circuit

AEC   Automotive Electronics Council

IDE   Integrated Development Environment

PIC   The name of a popular brand of microcontrollers made by Microchip

GUI   Graphic User Interface

INTRODUCTION

A brushless motor serves the same purpose as any other motor, to convert electrical energy into mechanical energy. There are a variety of devices that can fall into the category of motor and as such most can be used interchangeably in many applications that would require one. However, to optimize the function of a given motor driven system a particular motor could be better utilized due to its characteristics. It is beyond the scope of this project to describe the wide array of electrical machines and their particular uses, but a few will be discussed to give the reader a better idea of what makes a brushless DC motor unique.

1.1 Background

In a typical brushed DC motor, mechanical commutation is used to apply force on the rotor. In this process a voltage is applied across the brushes of the motor and, as the motor spins, current is provided through the physical contact of the brushes. At each occurrence of the brush passing the current to the rotor, the polarity of the rotor is reversed, which causes the attraction of the rotor to switch to the other side of the motor [1]. This process can be seen in figure 1 below. After the polarity changes in step 3, the next pole pair in sequence is energized so the magnet is constantly being pulled around in a clockwise pattern.

Step 1	Step 2	Step 3	Step 4
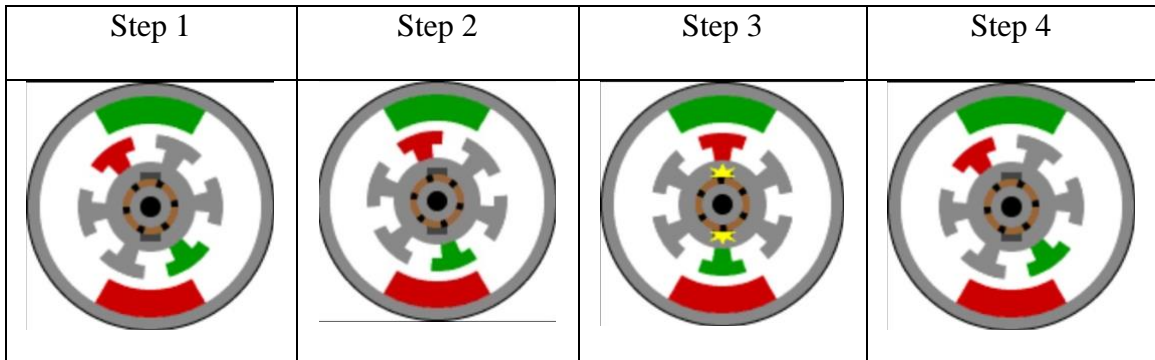
Figure 1. Brushed Motor Commutation Sequence [2]

This process of switching is called commutation and it will continue as long as a DC voltage is applied with no need for any other external elements. Due to the mechanical brush components, which provide the electrical contacts needed to drive the motor, brushed DC motors are subject to wear out over time. The brushes wear away over time and the commutator needs to be kept clean through regular servicing of the motor [3].

The main difference between the brushed and brushless DC motors is that the mechanical commutation performed by the brushes is replaced by a circuit of electrical switches. Some sort of controller, usually a small circuit board, is needed to coordinate when the magnets in the motor are energized in order to apply a rotational force on the rotor. In figure 2 below, a three-phase BLDC motor with three pole pairs is shown. The first four steps are shown but an additional two steps are needed to complete the standard six-step commutation process.

Step 1	Step 2	Step 3	Step 4
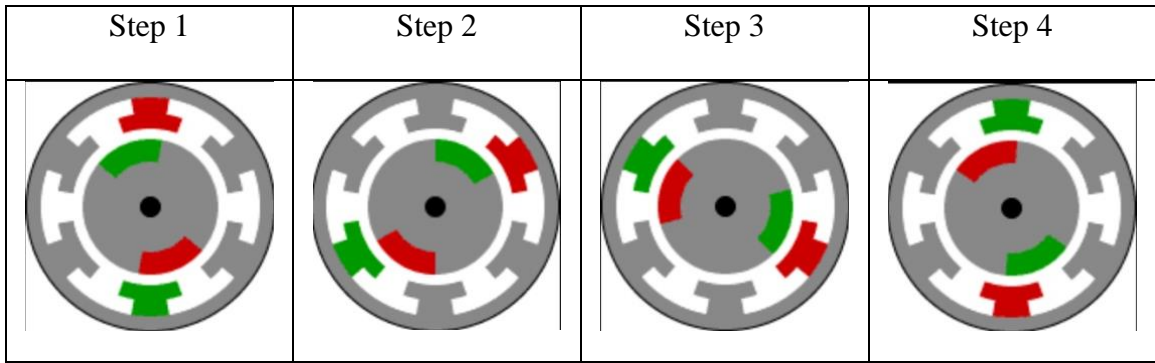
Figure 2. Brushless Motor Commutation [2]

At each stage of this commutation process, two pole pairs are energized while one pair is left open. By energizing these pole pairs in an appropriately timed sequence, the magnets will provide the necessary forces to push and pull the rotor into motion. A microcontroller type device is necessary to keep this timing and effectively drive the motor.

Brushless DC motors use a permanent magnet and can go by several other similar names including: permanent magnet synchronous machine, brushless permanent magnet synchronous motor, brushless AC motor, brushless DC motor, and permanent magnet servo motor [3]. However, the shape of the back EMF can be used to further differentiate the brushless motor from the permanent magnet synchronous motor. In a brushless motor, the back EMF is in the form of a trapezoidal waveform while the back EMF of a permanent magnet synchronous motor is sinusoidal [4]. Their respective shapes of the back EMF are shown in the figure below.
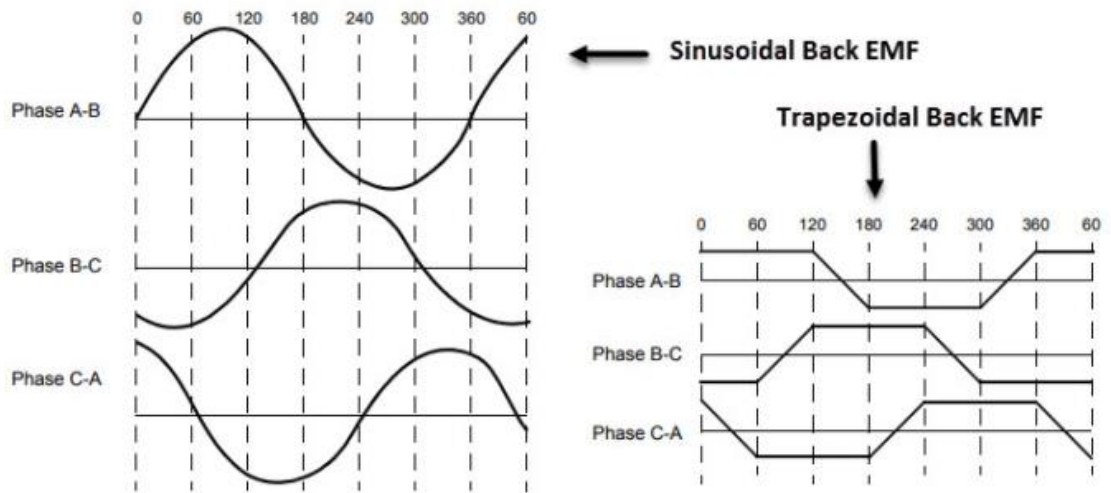
Figure 3. Sinusoidal and Trapezoidal Back EMF Waveforms [5]

As you can see a brushless DC motor operates as a permanent magnet brushed motor but with electronics taking the place of the brushes to perform the commutation and spin the rotor [4]. All these names can be confusing but are sourced from the fact that brushless DC motors are powered by alternating current while exhibiting several characteristics of a standard brushed DC motor.

Brushless motors began to take off with the innovations and accelerated development of microcontrollers and digital signal processors in the late 1990s. These devices make the electronic commutation much more feasible for the more practical implementation of brushless motors in a wide variety of industries [6]. The use of brushless DC motors has recently become increasingly common due to their better characteristics in comparison to their brushed counterparts [7]. These motors are currently used in a variety of applications including automotive fuel pumps, air blowers, and engine cooling fans. In

these cases and others, a sensorless brushless DC motor controller can simplify the overall system in which it is implemented while reducing the costs of other motor drive systems [7]. Brushless motors are "inherently more reliable, more efficient and with current electronics technology, more cost-effective than the standard brush-type fuel-pump motor and controller [7]." For example, dusty or oily environments or applications where it is difficult to reach the motor for maintenance would benefit from the use of a brushless DC motor [8]. In applications where performance is more of a concern than simplicity or reliability, the torque for a BLDC motor compared to a conventional motor is significantly higher which means the technology can be applied where size and weight are important factors [7].

Automotive manufacturers are beginning to choose BLDC's when possible because of their "greater control, improved efficiency, and higher reliability" compared to alternatives [9]. Recently, sensorless BLDCs have become a more popular choice because the removal of sensors from the devices lowers the cost of the system [9]. For example, in the automotive industry many vehicles use anywhere from a dozen to a few hundred motors in a given design. The use of the more efficient, higher reliability brushless motors has become more common as manufacturers strive for energy-saving and thus more environmentally friendly products [6].

Brushless motors are also becoming increasingly popular in the more hobbyist section of industry and are being used extensively in mid to high-end drones [10]. The electronic device used to control the motors in more hobbyist market segments often goes by a

different name but serves the same principal function as any other BLDC motor
controller. An electronic speed controller (ESC) takes power from a battery or other
external supply and sends the appropriate signals to drive the motor. In the figure below
the red and black wires are connected to a battery and the three blue wires control each
phase of the small three-phase brushless motor.

Figure 4. Example of a Hobbyist ESC for a Small BLDC [11]

1.2 Objective

Since a brushless motor is commutated entirely through an electrical system,
improvements of microprocessors and power electronics will always go hand in hand
with more improved and versatile brushless motor systems. Without further innovation of
these electronic control systems, the further use of brushless motors may be greatly

hindered. Current research topics surrounding the subject of brushless motors have been summarized to fall into three main areas by Xia in his book, Permanent Magnet Brushless DC Motor Drives and Controls:

1. The development of sensorless control technology to improve system reliability with the additional benefit of decreasing a given system's size and weight.

2. The exploration of new ways to reduce the torque ripple characteristics of brushless motors.

3. Innovation of BLDC motor controllers to be more reliable, compact, and versatile.

The objective of this project is to design and fabricate a printed circuit board based motor control system to drive a 3 phase brushless DC motor. The system is to be constructed with components robust enough to be used in automotive applications, be able to drive the motor with up to 24 volts inputted from an external power supply, and use a feedback loop closed with a sensorless method using a current sensing measurement technique.

LITERATURE REVIEW

This literature review begins by covering the differences between brushed and brushless motors. It is continued with the description of the most common control and feedback methods of brushless motor control systems, which will be reviewed and compared. The chapter will then walk through the three fundamental components of a brushless motor controller, moving through the system from the power supply to output power sent to the motor. The selection considerations of components for a potential controller design will be discussed along each step of this process. A short discussion on temperature considerations regarding the finished printed circuit board based system is followed by some circuit board design principles for improved thermal management. This chapter will then be rounded out by a review of electric motor properties and some performance metrics to be considered in the design portion of this report. The contents of this research into the various properties of a functional brushless motor system lays the foundation for a successful design and relevant analysis of the design's performance.

2.1 Detailed Comparison of Brushed DC Motors vs Brushless DC Motors

Despite their increased use in recent applications resulting from their greater control, efficiency, and reliability compared to their brushed counterparts, there are some disadvantages to brushless motors. This is especially true for applications where the goal is to be small and simple. It was found that in small devices, brushless motor controllers can become a source of inefficiency [12]. Another disadvantage of applying brushless motors to a particular use case is that a separate controller with relatively complicated electronics is needed [12]. In their paper, A Characterization of Small DC Brushed and

Brushless Motors, Harrington and Kroninger also point out that although the size and weight of the motor can be reduced, that may not account for the addition of the necessary controller. Despite some drawbacks, it was found that the small, cheap BLDC motors tested in Harrington's research performed at higher speeds with reduced electrical noise compared to similar brushed DC motors [12].

Similar statements about the drawbacks and benefits are made in other papers such as those written in Paul Pickering's article. Pickering states that brushless motors "have higher efficiency, higher torque to weight ratio, lower maintenance, higher reliability, and lower noise" compared to conventional brushed motors. It is stated that the major trade-off for these improvements is that brushless motors "require considerably more electronic circuitry to operate [13]."

Within the category of brushless DC motors, there are two dominant choices: Single-phase and three-phase. Although the single-phase motors are less expensive they have several tradeoffs including high electrical and acoustic noise, high ripple currents, and are typically less efficient than three-phase brushless motors [14].

2.2 Comparison of Overall Cost, Effectiveness, and Tradeoffs Between Sensored and Sensorless Methods of a Feedback Loop to the Motor Controller
Methods to measure the speed of the motor for use in a feedback loop are completed in one of two ways: Either by incorporating an external sensor into the motor drive system (sensored) or using a microcontroller to measure electrical signal resulting from the back

EMF of the motor (sensorless). Permanent magnet motors, such as a BLDC, require some sort of position sensing method to perform phase commutation and close the feedback loop to the controller. There are a handful of drawbacks that come with the addition of such a position sensor. These sensors can incur additional costs and require a larger motor size [7]. Extra components, such as the sensors, have to meet the operating environment requirements of the rest of the system while adding an additional component that has potential failures. This increase in the number of components decreases the overall reliability of the system [7]. These sensors are also often sensitive to high temperatures which limits the motor operation to temperatures below 75 degrees Celsius [15]. For these reasons, sensorless systems, which take electrical measurements through back EMF and current sensing, can prove to be a beneficial alternative to the addition of sensors on brushless motors.

There are other sensorless control methods, but the back EMF method is the most widely used and tested method for sensorless feedback. In this method the zero-crossing events are detected and used when a BLDC motor is driven with only two of the three phases at a time, leaving one phase open [6]. This de-energized phase is used to measure a voltage at zero-crossing events. A zero-crossing event occurs when the voltage between a neutral point of the three motor phases, and the de-energized phase is equal to zero. From this point, the voltage of the floating phase can be measured. The measured voltage of this undriven phase is proportional to the back EMF [16]. The back EMF of the motor is directly proportional to its speed so changes in speed can be measured via changes in the back EMF.

Of course, there are tradeoffs to be considered with the back EMF sensing method and there are a couple of significant challenges in using the method. The main challenge being the design of a system that is able to accurately sense the zero-crossing events. Another challenge is starting the rotation using the sensorless method because the location of the rotor position is unknown until the motor begins rotating and a back EMF signal is produced. Therefore, a preprogrammed open-loop starting sequence is often used before switching to the closed-loop sensorless control once a back EMF signal is detected and the feedback loop can be completed. Since motion is needed to produce a back EMF measurement, connected motors do not work well in lower speed settings. In an effort to overcome the challenges of sensorless systems, improved starting sequences currently remain a large focus of research in the field of brushless motor control drives [6]. In addition to the motor needing to move at a minimum rate to generate a measurable level of back EMF signal, the controller is sensitive to sudden changes on the load of the motor and speeds outside of the ideal commutation rate for the motor [17]. For some applications where low-speed start-up control is necessary, sensorless control is not the best method. However, if the system is not sensitive to this limitation, the benefits of a sensorless brushless motor controller are numerous.

2.3 Comparison of Sinusoidal vs Standard Trapezoidal Sensorless Control Methods and the Resulting Performance

There are two main types of inputs that can be sent to a brushless motor from the controller. Each of which has distinct technical challenges and performance

characteristics. Trapezoidal motor control is the simpler and more conventional method while sinusoidal and pseudo sinusoidal motor control can be achieved with more complex integrated circuit microprocessors.

In trapezoidal control, a six-step commutation sequence is used in which the phases of the motor are energized in a sequence that causes the rotor of the motor to spin. Current is sent through the motor one phase pair at a time with the remaining phase always left de-energized. This produces a current wave that appears in steps that change between positive, zero, and negative current. This pattern creates a roughly trapezoidal shaped waveform of the current applied in each phase over a given period of time [18].

In sinusoidal control, current is supplied to each of the three motor phases simultaneously. The current is varied in a sinusoidal pattern that is much smoother than the rough switching in the six-step trapezoidal commutation sequence [18]. This sort of commutation is complex and manufacturers of devices that include sinusoidal drive modes generally provide vague descriptions such as, "The DRV10983 device uses a proprietary sensorless control scheme to provide continuous sinusoidal drive [19]." Therefore, it is difficult to further describe how this commutation technique is achieved on a case to case basis in addition to how close the advertised technique is to true sinusoidal commutation as opposed to a pseudo sinusoidal method. However, the general effects of sinusoidal techniques are documented, and their results can be compared to those of trapezoidal commutation techniques.

The more standard trapezoidal control method is generally used for higher speeds

because at decreased speeds current ripples are created in instances where the current is

changed from positive to zero to negative. This ripple results in less than optimal noise

and uneven operation. Sinusoidal control negates this ripple effect [13].

For many uses trapezoidal control is all that is needed for the controller, but sinusoidal

control can improve efficiency, reduce noise, and improve the torque inputs. Sinusoidal

control is the best way to achieve a "smoother, more efficient, and quieter" operation of a

brushless DC motor [20]. Sinusoidal control methods can also be paired with a sensorless

BLDC motor controller [20]. While the use of a sinusoidal control method can increase

the cost and complexity of a system, the trend of better development tools and more

powerful integrated circuits makes a design for sinusoidal control increasingly feasible.

2.4 Component Selection

In a typical printed circuit board based brushless motor control system, three fundamental

sections are needed for the basic operation of a connected motor from a given power

supply. These include a microcontroller, a pre-driver, and a three-phase inverter. The

basic connections of these sections to an external power supply and motor are shown in

the figure below.
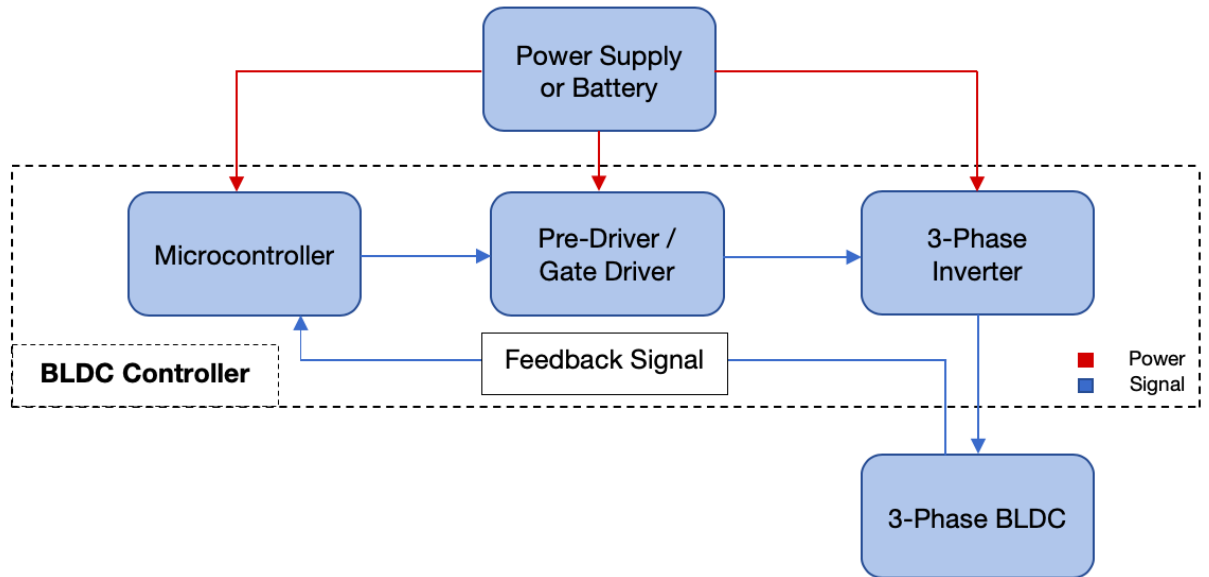
Figure 5. Diagram of Fundamental BLDC Control System

Often there are other additional sections that are relatively common. This includes

additional protective circuits, user interface circuits, and peripheral display circuits for

system status visualization.

Different integrated chip manufacturers produce a variety of functions bundled into

different packages that can be used to serve the requirements of each fundamental section

of the system. For example, Texas Instruments produces devices that combine a motor

driver with MOSFETs to drive the motor directly with an external microcontroller.

Another example is Infineon which produces a chip combining the microcontroller and

pre-driver to be paired with external MOSFETs. Feedback for the system is often

completed through the use of current sensors. The use of a sensor for each phase provides

current feedback to the controller but individual current sensors are not often needed

because they can be integrated into MOSFETS or other power switches and several

manufacturers make them in a variety of specifications [7].

Although there are several ways to combine packages of components currently available

on the market, the aforementioned three main functional areas are necessary to create an

operable brushless DC motor controller. These main components include a

microcontroller that is programmed to read and write signals, a gate driver to drive the

three-phase motor, and MOSFETs to deliver ample current to the motor. Ultimately, two-

in-one combinations of functions for integrated circuit components is commonplace

because a reduced chip count can reduce design time and cost. However, this comes with

the drawback of sacrificing design flexibility and in turn, potential performance [13].

2.4.1 Microcontroller

The use of a microcontroller in the motor control system is central to the function of the

rest of the circuitry. It executes the coded control programs loaded onto it, processes

feedback signals from other components in the circuit, and sends the appropriate control

signals to peripheral components to drive the motor. A variety of microcontrollers with a

wide range of performance characteristics make the selection decision of this core

component very important [6].

Some basic motor control schemes were developed after the introduction of pulse width

modulation based inverters but more complex control algorithms such as field-oriented

control require more complex processing and had to wait for digital signal processing to

become powerful and cheap enough to be widely used. Today, many DSP controllers are available that meet the requirements to be used within a high-performance motor control system [3]. Therefore, digital signal processing or DSP controllers are a main focus of interest in BLDC systems because of their ability to implement more advanced control software into a motor control system. Its use in combination with sensorless brushless drives can create much higher performance than standard controllers with separate position sensors [7]. Including a processor with DSP capabilities will allow a motor control system to be future proofed such that all hardware will be compatible with advancements of future software. This will allow for revisions that can enhance the performance without revising the original hardware design. High-performance sinusoidal control will require some form of DSP for calculations [21].

2.4.2 Motor Drives

As we continue through the structure of a BLDC control system, we move from the microcontroller to the motor drive. The purpose of the driving circuit in a brushless motor design is to receive the pulse width modulation signals from the microcontroller and provide power amplification to the motor according to the PWM signals. A gate driving circuit can come in several forms but serves the same general purpose in all microcontroller-based motor drive systems. Many solutions currently on the market bundle three gate drivers into one integrated circuit package. Called a pre-driver or gate driver, this device receives six PWM signals from the microcontroller. Three of which drive the upper MOSFETs while the other three drive the lower switches. This circuit can

come in a variety of forms. Most commonly these are the isolated gate driver, pre-driver, and motor driver.

The isolated gate driver amplifies PWM signals sent from an external source such as a microcontroller and relays them to a switching device such as a MOSFET to drive the attached motor. An example of this type of component connected to a MOSFET and a single-phase motor is shown below.
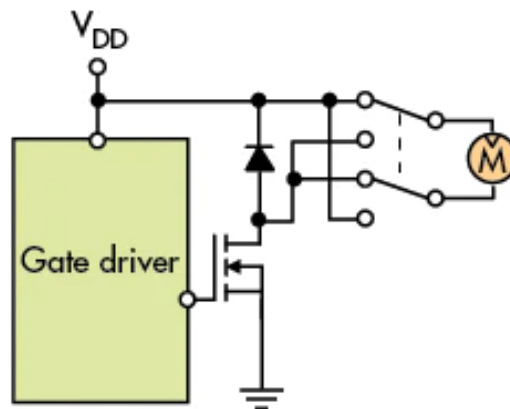
Figure 6. Isolated Gate Driver [13]

Multiple isolated gate drivers can be laid out in a trio to drive a three-phase motor with each component being connected to one of the motor's three phases. The internal structure of an isolated gate driver can be combined into a single package to drive a three-phase motor and is called a pre-driver or gate driver. A diagram of this component is shown below and is connected to six peripheral MOSFETs and a three-phase motor.
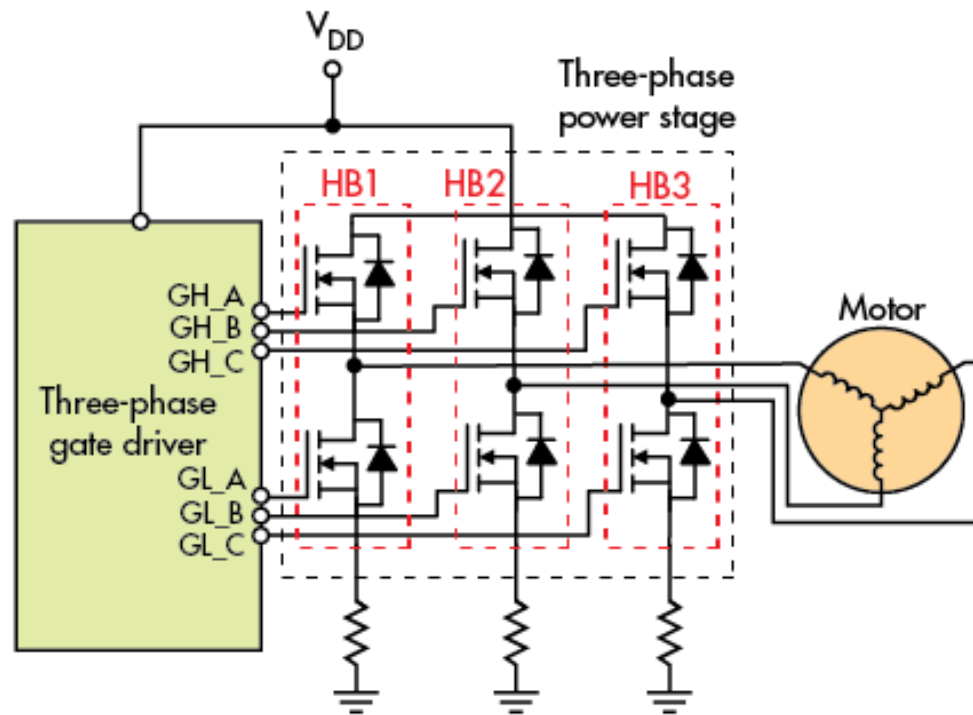
Figure 7. Pre-Driver [13]

There is another common combination of components to serve the purpose of a motor driver circuit that combines the internal structures of three isolated gate drivers and six MOSFETs into a single package. This device can directly connect a microcontroller and a three-phase motor. The functional block diagram for this type of device is shown below.
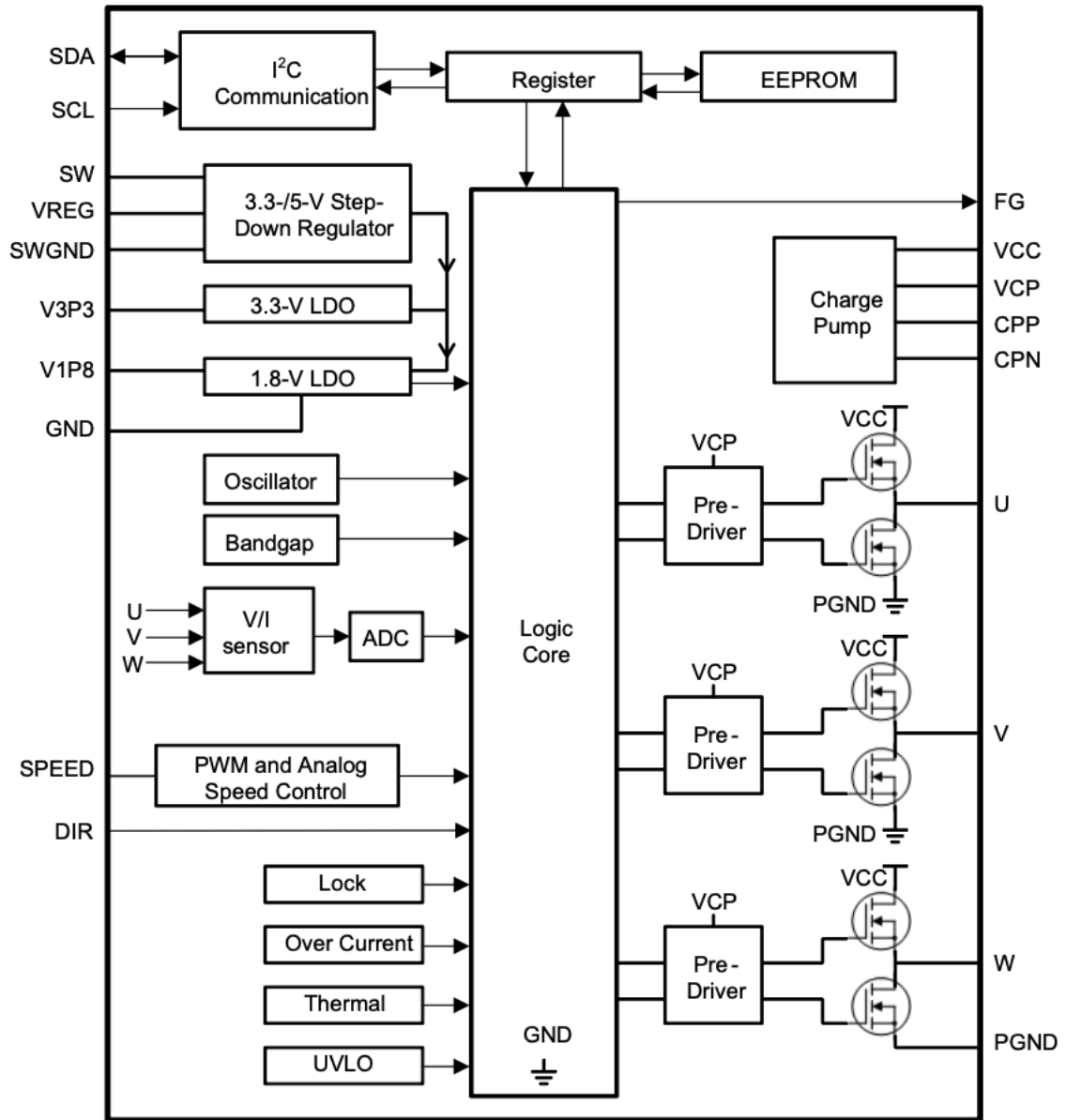
Figure 8. Motor Driver [19]

In this case, the SDA and SCL pins would connect the motor driver to a microcontroller using I2C communication and the U, V, and W pins would directly connect to a three-phase motor.

2.4.3 Three Phase Inverter and MOSFETs

We now progress through this section from the motor drive circuit to the MOSFETs that make up the power inverter that sends power to the motor. In order to produce a smooth speed control, a smooth variation of the power supply frequency is necessary. An inverter serves this purpose by drawing power from a constant voltage supply and converting it to a variable frequency of variable voltage to drive the motor. In the case of a three-phase motor, a bridge inverter is commonly used [3]. Bridge inverters usually have three phases and are made up of six MOSFETs or IGBTs [6]. Most low power three-phase inverters use MOSFETs while larger inverters tend to use IGBTs. The low to medium power inverters that MOSFETs are most often found are generally designed to handle up to 700V and a few kilowatts [3]. An example of a three-phase inverter composed of MOSFETs is connected to a brushless motor and shown in the figure below.
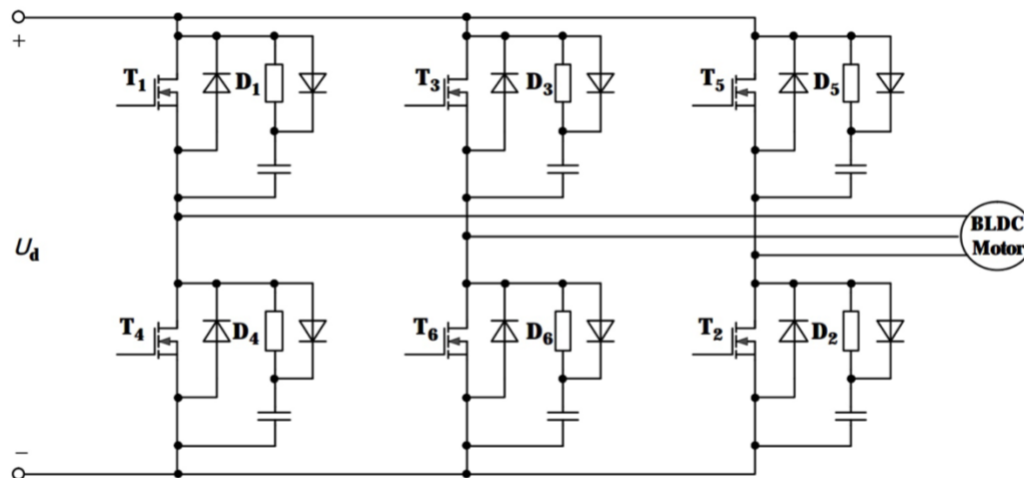
Figure 9. Three Phase Inverter [6]

Although they are the simplest component, the MOSFETs that make up the three-phase inverter are important factors in the performance capability of the motor control system.

Their characteristics are especially important because these devices deliver the current

necessary to drive the connected motor. The power created from this current is the factor

that ultimately determines the maximum mechanical output power of the motor. The

three-terminal MOSFET device is available in either N-Channel or P-Channel versions

[3]. The symbols for each are shown below.
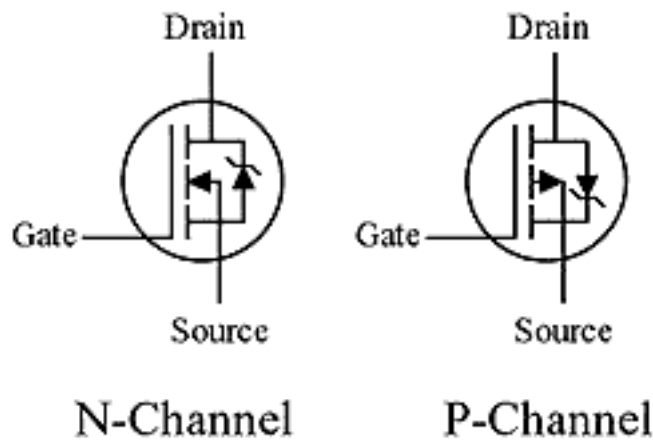
Figure 10. N-Channel vs P-Channel MOSFETs [22]

Proper consideration of the MOSFET's parameters will aid in assuring that the system

requirements are met. One important parameter to consider is a component's breakdown

voltage. A MOSFET with a greater breakdown voltage threshold will improve reliability,

providing protection against transients which can be introduced through other

components in the system. The necessary breakdown voltage needed for the system to be

protected can be determined by supply voltage to the system. For a system with a 12V

supply, a breakdown voltage of 40V would be sufficient while a breakdown voltage

rating of 60V would be needed on a system with a 24V power supply [9].

In a system like brushless motor control, efficiency is often indicated by how the devices in the system dissipate heat. Proper thermal considerations with the MOSFETs are important and especially necessary in high-temperature environments like those found in automotive applications. A couple of parameters are important in the selection of a MOSFET if good thermal management and thus improved efficiency is a goal. The on resistance or Rds(on) and the gate charge (Qg) have a great impact on a BLDC motor driver.

In similar sized MOSFETs, an N-Channel MOSFET will typically have an Rds of half the value of a P-Channel MOSFET. As a result, N-Channel MOSFETs are most often chosen for motor drive applications [9]. Overall, MOSFETs used in a motor drive system are an integral piece of the system's overall function and their characteristics can have a significant effect on the efficiency and performance of a BLDC motor [9].

2.5 Temperature Considerations with Regard to Printed Circuit Board Design

Electronic components dissipate power while operating, and as a result, experience a rise in temperature of the component. The greater the current that flows through the component, the greater the increase. Components can be damaged by significant increases to their internal temperature and management of an electronic device's thermal characteristics is important to its successful operation especially in the case of high-power circuits [23]. Heatsinks and forced air cooling are commonly used to manage thermal characteristics of a circuit board based device, but detailed circuit board design practices can also provide improvement to the thermal characteristics of a device. One

example is the strategic placement of components in optimal locations to improve heat dissipation [23].

While the addition of extra elements to cool an electronic device such as fans and heatsinks can provide a greater cooling effect than simply adjusting the placement of components, even a small improvement to the device's heat dissipation capability is important. In a study on the thermal reliability of electronic components on a PCB, it is stated that "when the device temperature is increased by 10℃, the failure rate of the equipments will probably increase a magnitude, so even reducing 1℃ in the electronics is very meaningful [24]." It has been found through simulation results that optimizing the placement of components on a PCB can affect the heat distribution and the thermal stresses on the device. Placing components in a more appropriate pattern can help to reduce the maximum temperature and thermal stress applied to the electronic components [24]. Some general guidelines include the recommendation that large power consumption components should be placed close to the edge of the circuit board and more heat-sensitive components should be located away from components that have a high power consumption [24].

In recent times, there has been a trend in the industry of power electronics components, such as MOSFETs, IGBTs, and high brightness LEDs, to miniaturize these components. This has been achieved all while still improving characteristics such as switching speed and current density [25]. The continued use and advancement of these smaller power electronics components is restricted by the capability of available thermal management

techniques. The power losses within the components create an increase in internal

temperature that must be dissipated away from the electronic device. Without proper heat

dissipation, the high temperatures can produce reliability issues to the component itself in

addition to the circuit board device as a whole [26].

Placing patterns of vias is an effective heat removal strategy for transferring heat away

from a hot component [26]. Doing so creates a relatively short conduction path through

the circuit board that can be seen in the figures below.
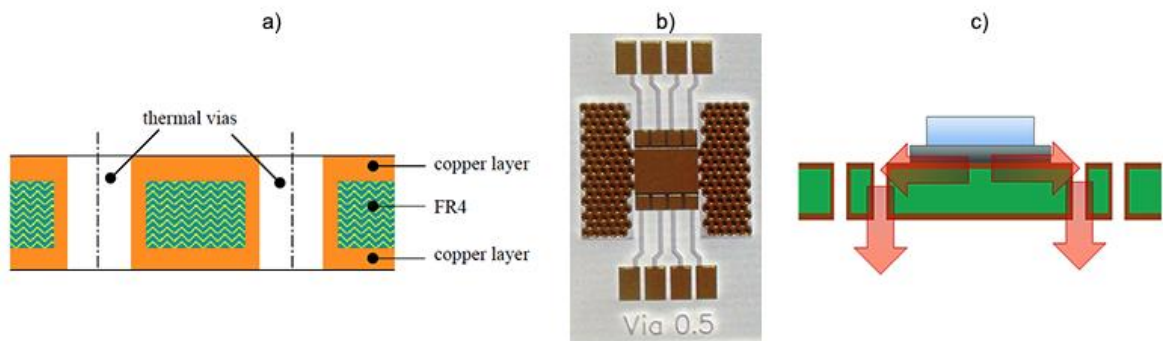
Figure 2. PCB with open thermal vias: a) Scheme; b) design; c) thermal path

Figure 11. Thermal Path through Vias [25]

Similar to the placement of components on a circuit board, the pattern in which the vias

are placed has a role in determining the effectiveness of the heat dissipation capability.

Other properties such as the diameter of the via and whether or not the vias are filled also

have an effect. One study has researched the optimal diameter for filled and non-filled

vias. It was concluded that for unfilled vias, the optimal diameter was .25 mm. This was

compared to the use of a .8mm diameter via which had a 44% greater thermal resistance.

For filled vias, the optimal diameter was found to be .2 mm. This was compared to a .8

mm via which had a 23% greater thermal resistance. In addition to looking at the optimal

diameter of the vias, this study found that the placement of vias in an offset pattern seen

in figure 12 and solder filling of vias contribute to reductions of thermal resistance [26].
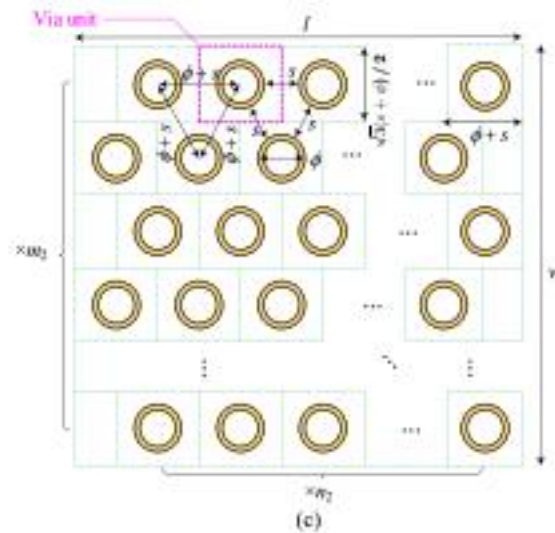
Figure 12. Diagram of Vias in Offset Pattern [26]

The importance of the via to via spacing factor is corroborated in a design of experiments

study attempting to optimize the thermal resistance of a PCB based on several factors laid

out in the figure below.
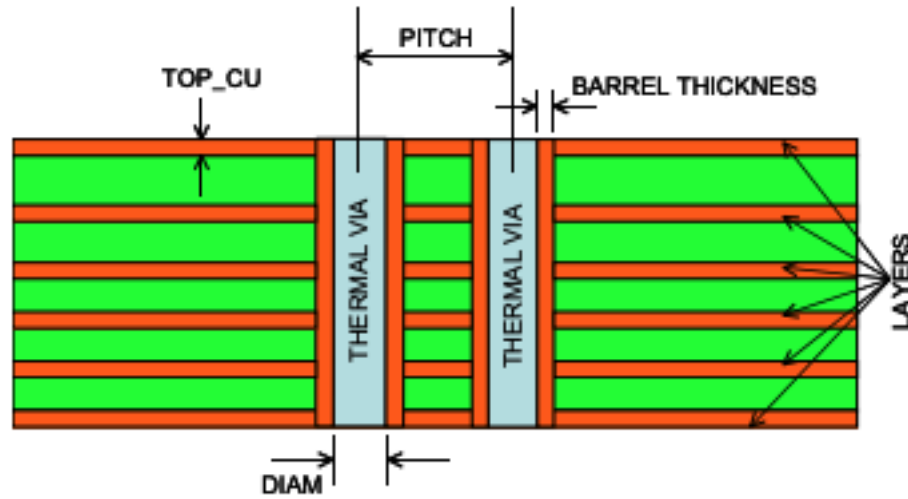
Figure 13. Diagram of DOE Factors [27]

It was concluded that to decrease the thermal resistance of a multilayer circuit board, a designer should decrease the pitch distance between vias, increase the copper barrel thickness, and increase the number of metalized copper layers. The distance between vias (pitch) was the most significant factor [27].

2.5.1 Engineering Standards

It should be mentioned that with the trend of miniaturizing high power consumption components there are commonly used standards and classifications to help designers choose components that remain reliable under high thermal stresses. Temperature standards for integrated circuit devices are generally categorized into three main categories summarized in the table below.

Table I. Temperature Standards by Category

Category	Temperature Range
Commercial	0 to 70 degrees Celsius
Industrial	-40 to 85 degrees Celsius
Military	-55 to 125 degrees Celsius

There are exceptions including automotive ratings in the range of -40 to 125 degrees Celsius among other non-standard ratings [23]. These ranges are broadly accepted but ultimately it is up to the manufacturer to determine how they grade their devices. In some cases, components are qualified through the Automotive Electronics Council who then tests the device based on their Q100 standards for packaged integrated circuits. The corresponding qualification test provides a 0 to 3 operating temperature grade for the given device. Details for the AEC temperature grading scale from the most recent 2014 publication are shown in the table below.

Table II. AEC Temperature Grading Scale for Q100 Standards [28]

Grade	Ambient Operating Temperature Range
0	-40 to 150 degrees Celsius
1	-40 to 125 degrees Celsius
2	-40 to 105 degrees Celsius
3	-40 to 85 degrees Celsius

Additionally, the AEC tests passive components under their Q200 standards. Details for the most recent temperature grading scale from their 2010 publication is shown in the table below.

Table III. AEC Temperature Grading Scale for Q200 Standards [29]

Grade	Temperature Range (degrees Celsius)
0	-50 to 150
1	-40 to 125
2	-40 to 105
3	-40 to 85
4	0 to 70

2.6 General Properties of Electric Motors and How to Improve their Output

Despite a range of varieties of motors available, electric motors all share very similar properties because their function is governed by the same physical laws [3]. For example, a motor's efficiency is proportional to its speed. A motor will run at a greater efficiency if it is operating at a higher speed. At a constant torque, power also is proportionally related to speed and therefore, higher speeds will produce a greater power output [3]. Any motor will produce more power if the electric circuit in the motor driver allows an increase in current supplied to the motor. The limiting factor in how much current can be supplied to the motor is how much temperature increase the hardware of the motor itself can sustain [3].

Maximum speed is determined by maximum voltage while maximum torque is determined by maximum current. The maximum current is set based on the allowed thermal increases of the conducting material in the motor itself. This restriction introduces the question of what power output could be achieved if this physical limiting factor were not considered. To answer this, we begin with the definition of a given motor's mechanical output power which is torque multiplied by speed. The resulting power when either of these terms is zero is no power and there exists a maximum power between the two zeros at half of the no load speed. This means that the back EMF produced by the motor is exactly half of the voltage produced by the supply[1]. This can be visualized in the figure below where V is the voltage provided to the motor, R is the resistance of the armature of the motor, and E is the back EMF produced by the motor.
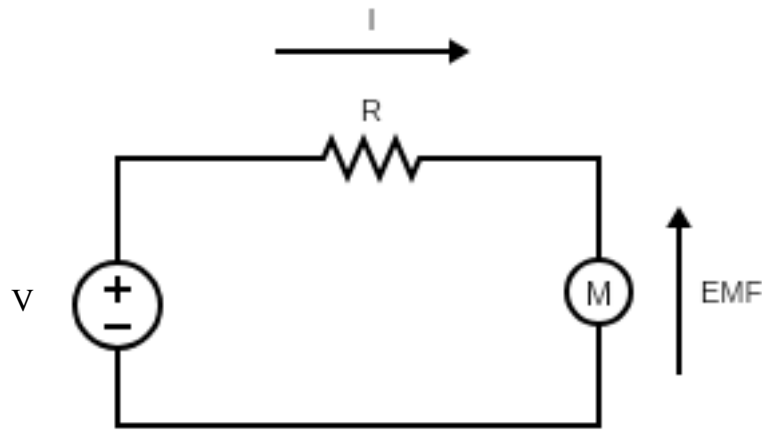
Figure 14. Equivalent Circuit of a DC Motor

---

[1] EMF = 1/2V

At maximum power the current is equivalent to V/2R and the mechanical output power is V2/4R.

$$Power_{max} = \frac{V^2}{4R}$$

It is stated that the use of this equation is purely of "academic interest" because it is only theoretically possible [3]. Of course, operating at maximum power reduces the efficiency of the motor which is limited to 50% because half of the available power is lost as heat in the armature resistance.

The energy efficiency of a motor is derived from the amount of mechanical output the motor can achieve based on its electrical input. The input power is the electrical input in watts and the output power is the torque multiplied by the rotational speed of the motor shaft in radians per second [30].

$$\eta = \frac{P_{output}}{P_{input}} = \frac{T \cdot \omega}{P_{elec}}$$

Another factor worth mentioning regarding the performance of electric motors is the torque ripples often created through many commutation techniques. Torque ripple reduction is a significant limiting factor in brushless motor controller systems [6]. During trapezoidal control, torque ripple and current spikes occur at each commutation point. The ripple leads to a reduction in the motor's efficiency [10]. Since torque ripple is an

inherent property of brushed DC motors and difficult to reduce or remove in its entirety, it is not to be considered in applications where a low torque ripple is desired. In applications like fans and pumps where the motors are run mostly at high speeds, the torque ripple has less of an adverse effect on the motor drive system [4]. The torque ripple conundrum is of enough importance to note, but Xia states, "speed and torque ripple are always problems that require further solution."

2.7 Summary of Literary Research

Overall a brushless motor control system is composed of hardware and software subsystems. The hardware system is made up of a microcontroller, motor driver, and a bridge inverter. The software portion of the system can be configured using either sensored or sensorless feedback loops. Sensorless control of a brushless DC motor can reduce cost and increase reliability in comparison to sensored systems. Sensorless control can be the only option when high performance is necessary in a harsher environment [7]. Furthermore, sensorless control can be completed using various control methods from the simpler trapezoidal method to the more complex sinusoidal methods.

In order to improve the performance of a motor, the controller must be designed to meet requirements created by the physical properties of electric motors. To meet these requirements, special considerations of the hardware design of a PCB based controller are required so that the physical restrictions of the motor itself is the main limiting factor to an increase in performance. These considerations include careful part selection, thermal management techniques, and proper circuit board design.

SYSTEM DESIGN

The system in this project was designed based on the basic structure of a BLDC controller described in the previous chapter. The core components receive power from either a battery or another external power supply. The BLDC controller also accepts user inputs that are sent to the microcontroller which, acts as the central component of the overall system. The microcontroller outputs an appropriate signal to an external motor driver that drives an array of MOSFETs arranged into a 3-phase inverter. These MOSFETs then deliver an amplified signal to the three-phase BLDC motor. The microcontroller also receives feedback information from the motor which is then used to adjust the signals sent to the motor and ultimately provide smooth control. A diagram of this structure is shown in the figure below.
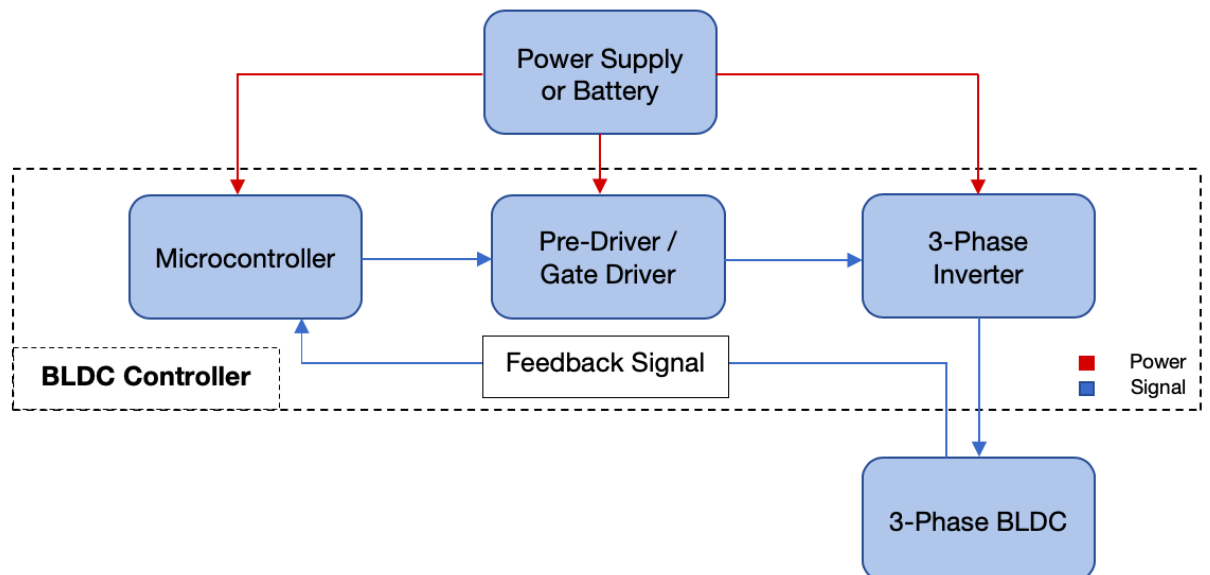
Figure 15. Diagram of a Fundamental BLDC Control System

The motor control system was designed to meet several requirements including the following:

- The system shall drive a selected motor with 24 volts as the input power

- Maximize the potential power delivered to the motor

- Incorporate a sensorless feedback loop

- Provide a smooth control to the motor

- Be designed to withstand ambient temperatures 90-125 degrees Celsius

The resulting physical construction of a device through this project is intended for the production of a single unit for concept testing and the resulting design was created with the intention of soldering all components by hand.

3.1 Initial Design

In the initial design for this system, the BLDC controller was divided into three main sections. A core component makes up the heart of each of these sections. A microcontroller, a pre-driver chip, and the six MOSFETs which compose the three-phase inverter serve as the core components in this design. Of course, the inclusion of passive components such as resistors, capacitors, and diodes within each of these sections is necessary for the complete functionality of the system.

3.1.1 Microcontroller Selection

In this design, the microcontroller is central to the overall function of the system. It is responsible for translating user input signals into electrical signals to operate the motor in

addition to sensing feedback signals and making adjustments to output signals. However, the chip chosen cannot serve these functions automatically, it must be programmed to serve its desired function. Therefore, the selection of a proven, easy to use microcontroller with extensive previous application was considered to be advantageous in comparison to a more technologically advanced controller. This consideration was a primary factor in the selection process of a microcontroller.

The PIC brand of microcontrollers produced by Microchip is a popular type of microcontroller from a large brand with a long history of successful use by both the hobbyist and commercial industries. There are a variety of PIC controllers to choose from and many of the newer PICs have Digital Signal Processing features built-in that would be needed for more complex motor control methods such as field-oriented or sinusoidal control. Several models are even designed for the purpose of motor control. With the selection of the PIC controller also comes an extensive library of application notes for motor control provided by Microchip and a development environment that is available for all types of computers (Windows, Mac, Linux). Additionally, microcontrollers in this family have been used successfully in previous studies on brushless motor controllers including a study on the performance of sinusoidal vs square wave supplies [31].

The specific PIC microcontroller chosen for the design was the dsPIC33FJ32MC204. This is one of the PIC controllers offered specifically for motor control and has pins designated for six PWM signals to command a separate motor driver. Additionally, it contains a DSP engine and meets the temperature requirement of 125 degrees Celsius. A

draft schematic of the microcontroller section of the initial design is shown in figure 16

below. The connections to the motor driver in this design, in addition to the feedback

signals from the motor, can be seen on the right side of the microcontroller.
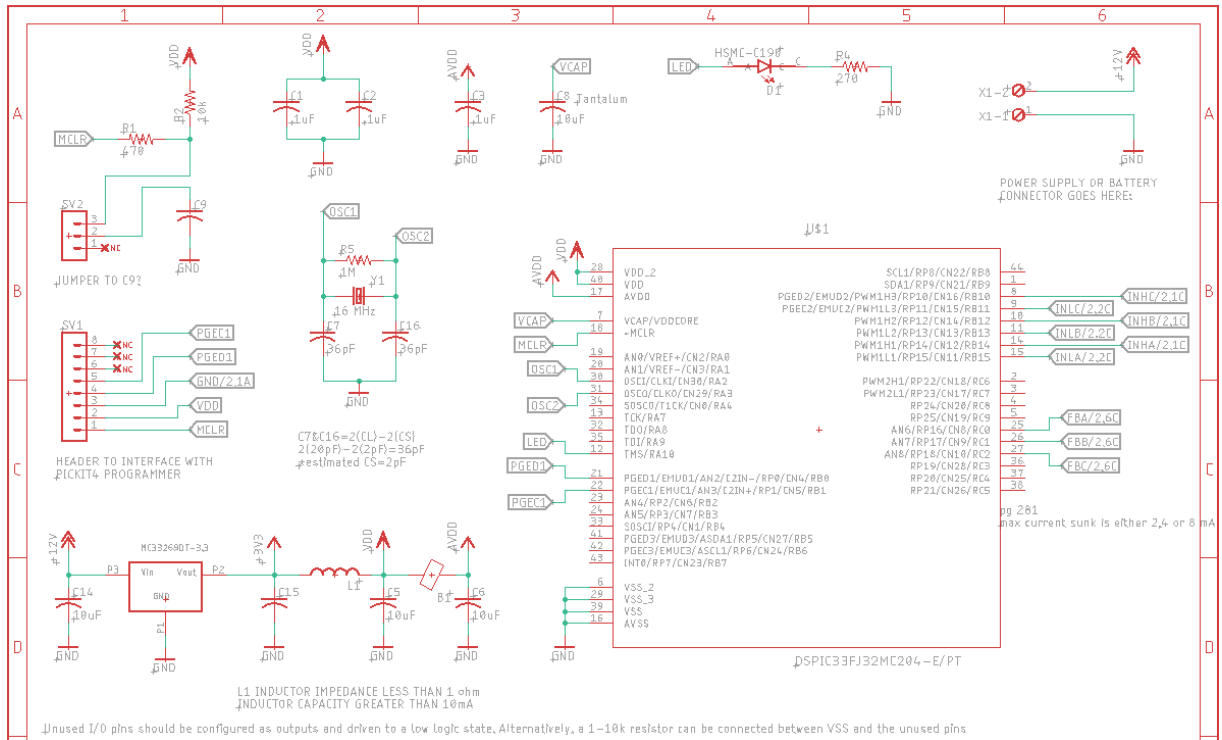
Figure 16. Draft Schematic of Initial Design – Microcontroller

3.1.2 Pre-Driver Selection

The difference between a gate driver or pre-driver compared to a motor driver is whether

the MOSFETs are internal to the integrated circuit's package or require an external

connection. In the pre-driver chips, external MOSFETs are used. Although the choice of

selecting a pre-driver over a motor driver IC sacrifices board space and the user-

friendliness coming from the inherent simplicity of single-chip integration, this sacrifice

allows the flexibility of choosing MOSFETs that more closely align with the design

goals. In this case, the flexibility allowed for the selection of MOSFETs that are capable

of delivering a much higher current to the motor. This can be compared to commonly

available motor driver ICs on the market which typically only deliver about 2 amps of

output current to the motor. Some examples of potential pre-driver selections are shown

in the table below.

Table IV. Comparison of Potential Pre-Drivers

	Microchip MCP8024	TI DRV8323R	NXP MC33937
Price	$2.80	$4.44	$6.54
Output Current	.5 A	1-2 A	1-2.5 A
Voltage Range	6-28 V	6-60 V	6-58 V
Operating Temperature	150 C	150 C	135 C

Although each of the listed IC's meet the basic requirements of the system, the Texas

Instruments TI DRV8340 was selected. This chip was similar to the DRV8323R listed in

the table but is more robust and is certified for automotive applications. The TI chip

allowed for the greatest ambient temperature tolerance and voltage input in the

comparable price range of pre-drivers considered. Additionally, TI maintains a positive

reputation for their motor driver chips and produced more easily navigable datasheets

than other manufacturers.

The DRV8340 is a three-phase gate driver designed for use in automotive applications in 12-24V systems. The chip allows for 6x, 3x, 1x, and independent PWM modes that are configured depending on which of the two versions of the DRV8340 is used. The 'S' version has its PWM mode configured through an SPI interface that connects to a microcontroller. On the other hand, the 'H' model is configured through the addition of resistors which permanently sets the PWM mode. In this design, the hardware ('H') version was chosen to reduce programming complexity. Its basic connections to the MOSFETs can be seen in the draft schematic in figure 17. Also shown here are the connections to the microcontroller which are located on the left-hand side of the pre-driver.
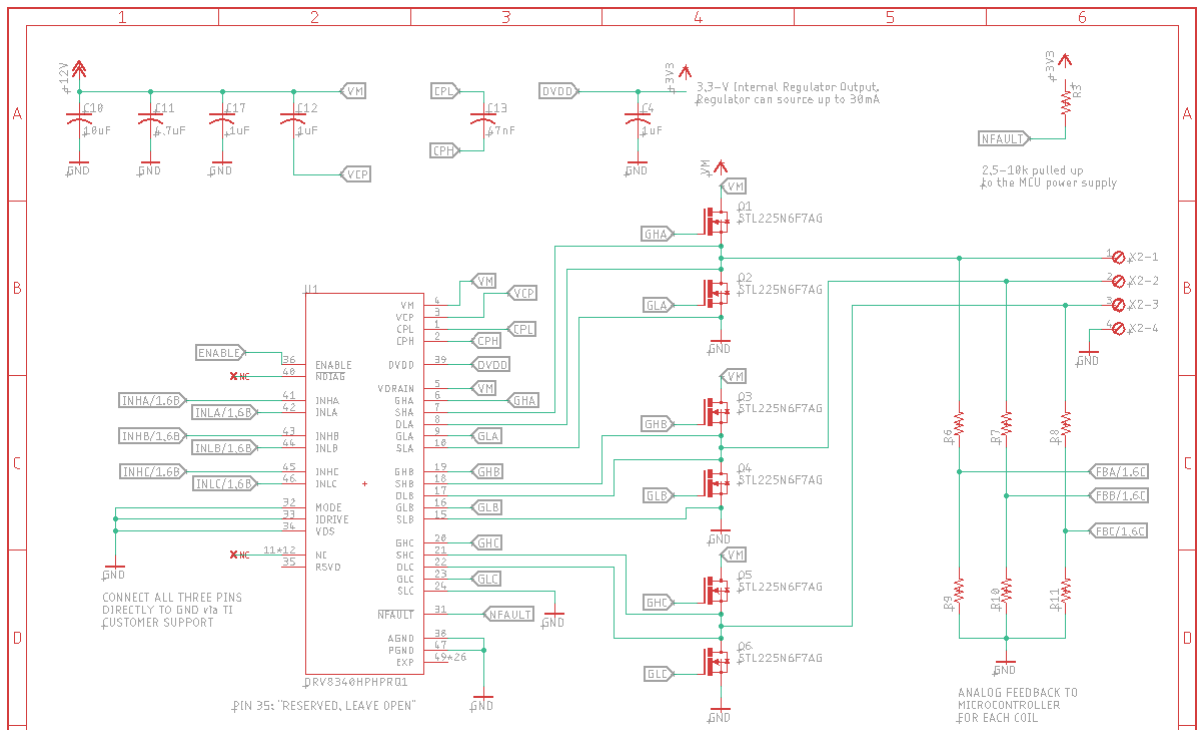

Figure 17. Draft Schematic of Initial Design - Motor Driver

3.1.3 MOSFET Selection

Several MOSFET types were considered for the three-phase inverter. Some options included power blocks, which combine the high and low side MOSFET into a single package. This design would only require three components, consume less board space, and ultimately simplify the design. When looking into specialty packages like the power block, there were limited options in regard to the range of important electrical characteristics such as low Rds, output current, and temperature requirements compared to the wider range of standard MOSFETs. To narrow the wide range of potential selections, MOSFETs were filtered to provide a large current output and meet automotive grade temperature requirements. The MOSFETs in the following table were examples of devices under consideration.

Table V. Comparison of Potential MOSFETs

	STL285N4F7AG[2]	BUK961R6-40E,118
Rds	1.1 mohm	1.36 mohm
Vds	40 V	40 V
Id	120 A	120 A

The MOSFET chosen to make up the three-phase inverter in this design was the STL225N6F7AG. This component has a very low Rds value of 1.4 mOhms, allows for the production of up to 120 amps, and has a breakdown voltage of 60 volts. As discussed previously, the greater breakdown voltage of the ST225 is more suitable for a 24V motor

---

[2] It is important to note that the ST MOSFET in the table above is not readily available in lower quantities while the BUK MOSFET widely available in order quantities as low as one.

supply system. This component is also AEC-Q100 qualified for an automotive grade system.

3.1.4 Schematic

The schematic for this initial design was created using Autodesk Eagle and included all supporting circuitry necessary for the basic operation of each component. It included screw terminal connections for an external power supply and three-phase BLDC motor. It used an eight-pin header designed to plug into the Microchip PICkit4 programmer that was to be used to load software on the system. It also included a 3-pin header designed to use a jumper to change the connection to allow for a change between programming and non-programming use modes for the microcontroller. Also included was an external crystal oscillator, a linear regulator to step down the 24 V supply to the 3.3 V microcontroller operating voltage, and an indicator LED that was intended to signal fault detections. Additionally, the design included a current sense resistor network that was intended to provide sensorless feedback of the motor to the microcontroller. The resistors remained unsized while developing supporting software. The footprints for each of these devices were sourced from included Eagle design packages or downloaded from SnapEda. This schematic was a preliminary draft of the initial design and many alterations and revisions were expected based on continued learning through later development work.

3.1.5 Development (Work with Microchip Development Board)

The creation of the schematic was the first step for the physical design of the system.

Before finalizing the design and laying out the circuit board, a development board was

acquired. The purpose of this was to begin the process of learning to program the selected

microcontroller in addition to the observation of a functioning system's operating details

and to discover missing elements in the project's design or shortfalls of the development

board system that would be improved upon through this project.

Due to the choice of the PIC microcontroller, the Microchip MCLV 2 development board

was selected. The development board works with the Microchip's MPLABX

development environment and a software development tool called motorBench for

automatically measuring a connected motor's parameters and generating appropriate

source code. Microchip additionally offers a physical plug-in module to test the

dsPIC33FJ32MC204 microcontroller with the MCLV2 development board. It was

planned to use this development board alongside Microchip's motorBench plugin as a

jumping-off point to be able to test software on functioning hardware. It was thought that

the motor control source code and documentation provided by Microchip would allow for

the creation of software that could be ported over to the custom designed circuit board for

final testing.

However, upon the receipt of the MCLV2 development board there were a few issues

that ultimately restricted its planned use. Three different paths were attempted to operate

a brushless DC motor using the development board with the MPLABX development

environment. The first two methods were attempts to load source code files using two different sensorless control techniques recommended and provided by Microchip for the MCLV2. The other and preferred path was using the motorBench plugin within the MPLABX IDE. After numerous technical issues using the development suite and unsuccessful resolution of said issues through manufacturer support networks, progress on this solution path stalled. After the limitations of this original design had become evident, the discovery of an alternative design path led to the abandonment of the design in favor of a more promising route.

3.2 Design 2

The second system design was built around the discovery of a programmable type of gate driver from Allegro Microsystems. The Allegro A4964 motor driver included additional features that allowed for the reduction of the learning curve required of programming a system from scratch. An available software package allowed for the monitoring of a variety of data points regarding the status of the motor. Additionally, the software allowed for the use of a settings menu in the user interface to make simple changes to the chip's firmware settings such as whether the driver was operating in trapezoidal or sinusoidal mode. Features like these allowed the PCB design, fabrication, and performance testing of the device to return to being the main focus of this study.

With the Allegro pre-driver, programming the sensorless feedback based on the current sense resistor network was no longer necessary. The Allegro chip includes internal systems to complete the collection and calculation without this external network. This

feature allows for a reduced part count and a decrease in programming complexity for the

system. Overall, the application of the A4964 IC changes the basic structure of the BLDC

controller. This can be seen in a revised block diagram of the system design in the figure

below.
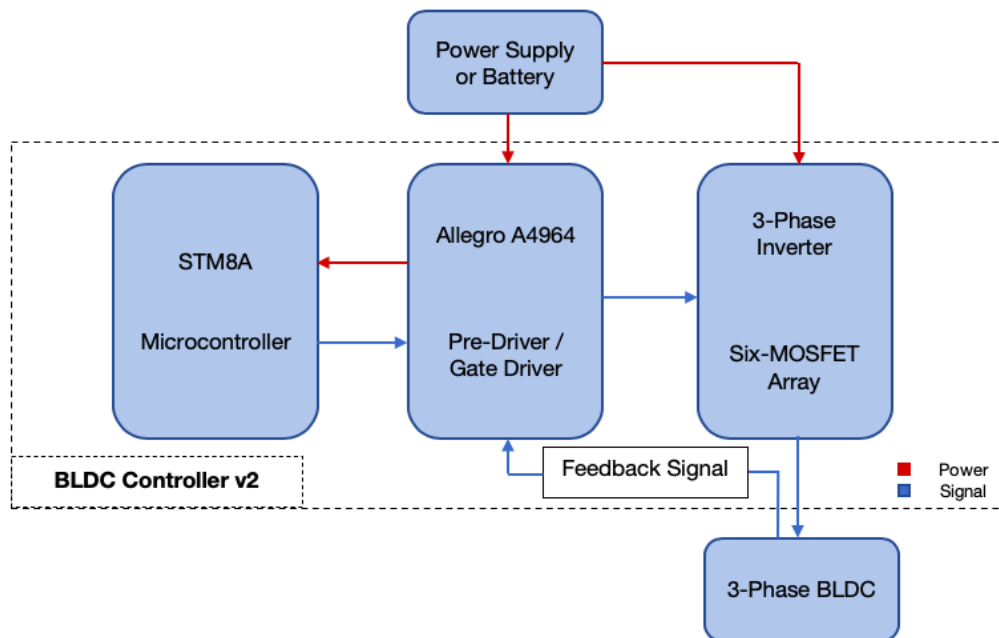
Figure 18. Diagram of Core Components of Design 2

In this set-up, the power for the microcontroller is supplied by the A4964 pre-driver

which acts as a voltage regulator and sends the voltage necessary to power the

microcontroller through the component's VLR pin. Through this connection, the A4964

can provide power to a microcontroller at either 3.3V or 5V as long as the current

remains less than 70mA. It should also be noted that the feedback signal from the motor

is sent directly back to the pre-driver without any intervention by the microcontroller.

3.2.1 Selection of Core Components

The selection process for each of the core components is detailed along with a description of the component ultimately selected for use in Design 2.

The A4964 is a sensorless motor controller capable of driving an external three-phase bridge of N-Channel MOSFETs through several drive modes including sinusoidal and trapezoidal settings. In the A4964 datasheet, Allegro states that their trapezoidal mode produces the highest output with a greater torque ripple while sinusoidal reduces the audible noise produced by the motor and the torque ripple outputted to the motor. The rotor position for each of these sensorless driving methods is found through the measurement of the back EMF produced by the motor. In trapezoidal mode, the position of the motor is found by detecting the zero-crossing point in the phase which is not currently driving the motor. However, while operating in sinusoidal mode, all three phases are constantly driving the motor so turning off a phase to detect a zero-crossing point is not possible. To overcome this limitation the A4964 stops producing signal for a short time where the crossing point is expected. The length of this detection period window is a setting that can be adjusted through one of the device's registers. Since the A4964 operates purely under sensorless operating methods, a startup sequence is required to start the motor before the back EMF can be sensed thus, initializing the control. Some key variables regarding this start-up sequence can be configured.

The A4964 can also be programmed to be operated by voltage control, current control, and closed-loop speed control methods. The chip also includes diagnostic detections for faults for under voltage, over temperature, and three-phase bridge faults. All these aforementioned control settings are adjusted by configuring registers of the A4964 through a small external microcontroller via the SPI communication interface. This four-wire hardware interface is provided to communicate with a microcontroller through an SPI port. The first three wires send information to set the registers of the A4964 and ultimately control the device. The fourth wire is used to feedback information through the readback register. This register can provide several types of information about the status of the system including the following:

- Diagnostic Codes

- Motor Speed

- Average Supply Current

- Supply Voltage

- Chip Temperature

- Demand Input

Besides the external three-phase bridge and small microcontroller, it is also required that the A4964 be connected to the main power supply through a reverse protection circuit and decoupled with ceramic capacitors. The combination of these external electronics is necessary for the operation of a connected BLDC motor.

Since the motor driver selected is a more advanced device, the needs for the microcontroller functions become far less demanding. The role of the microcontroller in the system is now mostly reserved for simple tasks like sending and receiving basic commands from the user over the SPI interface. As a result of this change, the microcontroller no longer needs powerful features like Digital Signal Processing that were included in the PIC microcontroller selected for the initial design. For the updated design a less powerful, 8-bit, PIC was initially considered but an 8-bit microcontroller from ST was ultimately selected. Some characteristics of each device can be compared in the table below.

Table VI. Comparison of Potential Microcontrollers

	PIC18F26K83	STM8AF6223
Price	$2.37	$1.89
Maximum Temperature	125 °C	150 °C
AEC Q100 Certified?	No	Yes

Notably, the STM8AF features a greater operating temperature tolerance at a significant reduction in cost. The specific STM8AF initially chosen was the 20 pin TSSOP package type. This device is capable of connecting to the A4964 pre-driver through SPI communication. It has enough ports to support a few auxiliary components such as a temperature sensor and connections to support some external control inputs from a potential user. After final code compilation it was discovered that the STM8AF6223 did not have sufficient flash memory available in an uncompressed file format. Since no

testing was feasible to validate the use of the compressed executable C code file, the STM8A microcontroller was upgraded out of caution to the STM8AF6266 to allow for greater storage capacity.

In this updated design the previous MOSFET choice for the 3-phase bridge was changed to the ON Semiconductor NVMFS5C604NL as a result of concerns over the current rating. It was desired that the current rating be three times that of the maximum applied current. The current rating from the ST MOSFETs of the initial design was increased from 120 A to 287 A in the new design. The footprint remained of similar size, the Rds was of similar range, and the breakdown voltage remained at 60 V. This device was also AEC-Q101 qualified for use in an automotive environment.

3.2.2 Additional Sections of Design 2

In the new system design for the BLDC, some additional sections were included in the system design. These include the design of an additional auxiliary circuit board with the purpose of programming, a temperature sensor, ports and supporting circuits for external inputs such as Analog and PWM commands, and protection and power filtering circuitry. A diagram showing these additional sections and their connections to the core components of the motor controller is shown in the figure below.
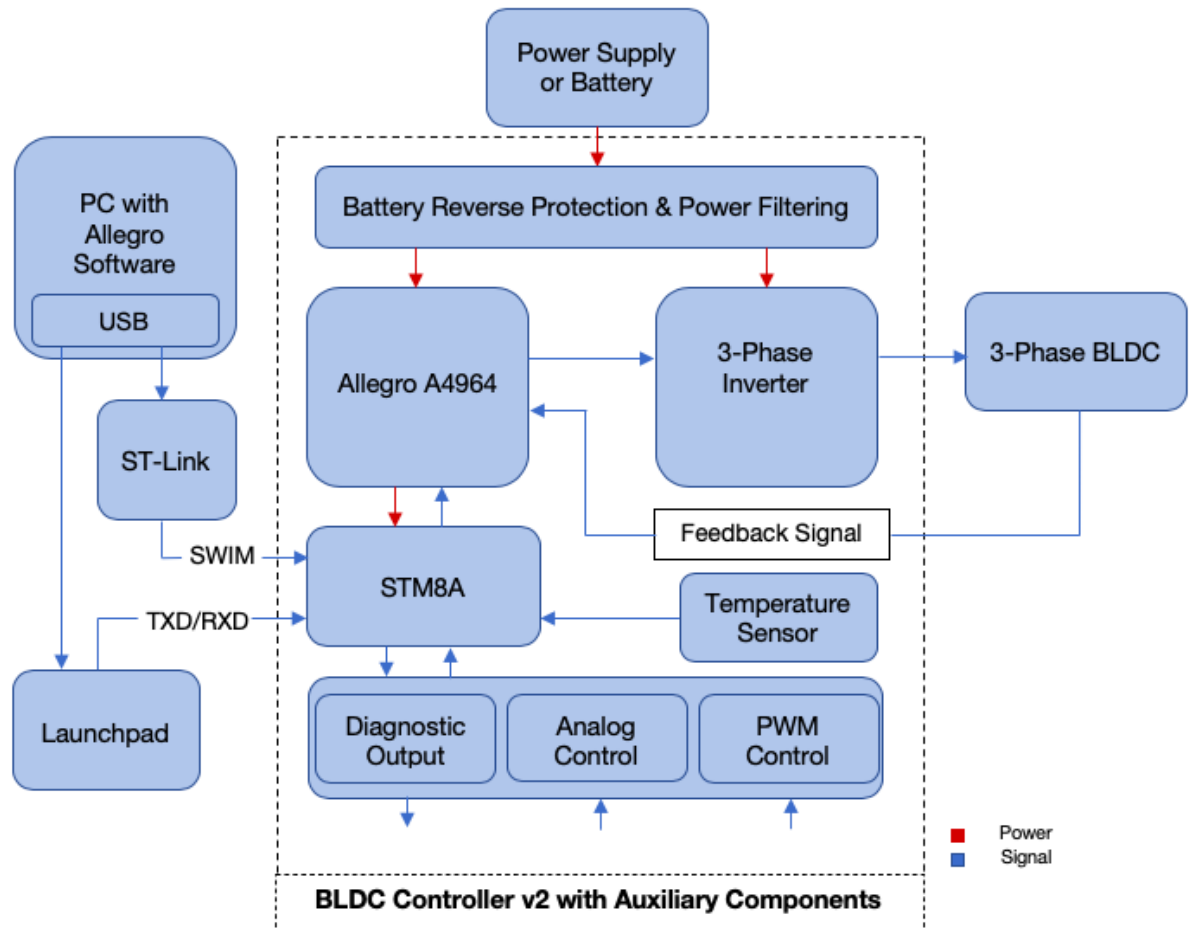
Figure 19. Diagram of BLDC Controller Design with Auxiliary Components

When designing the main circuit board, it was decided to separate the PC to

microcontroller programming circuitry from the main board and allow two ways to

program the ST microcontroller. The first of which is through the SWIM connection

using the manufacturer recommended programmer called the ST-Link. The second,

alternative programming method, was of a custom design using a USB to UART chip.

This alternative method would function similar to the onboard USB to UART circuitry on

the Allegro development board. This auxiliary device was named Launchpad and

included a micro USB port, an MCP2200 USB to UART chip and TXD/RXD header pins

to connect to the main circuit board via a ribbon cable.

To avoid the use of an exposed board a simple enclosure was designed for the device. It

was comprised of two interconnecting pieces. The circuit board would contain four

mounting holes on each corner that would align with the four pins in the bottom piece
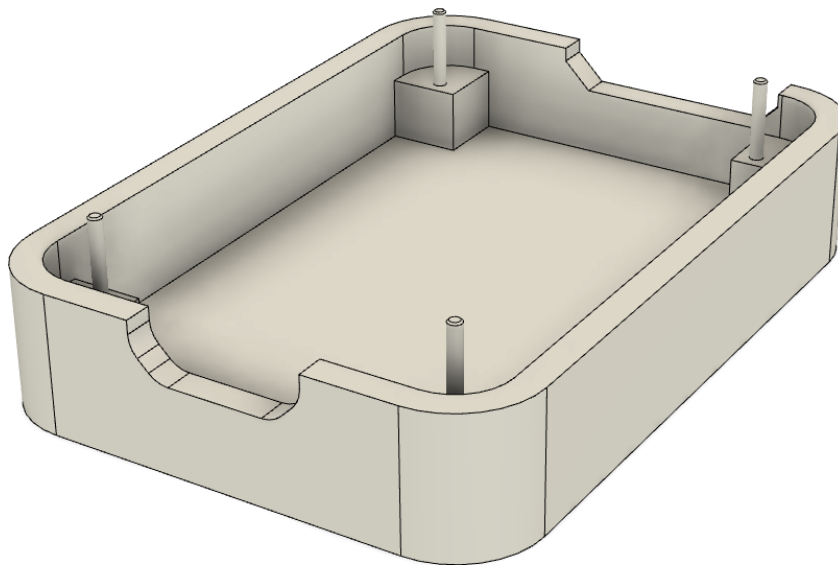
shown below.

Figure 20. Bottom Piece of Launchpad Enclosure

The board would then rest on the four pads that extrude up from each corner and allow

for the board to be raised off the bottom of the enclosure. The bottom piece of the

enclosure is designed for the four pins to fit through the mounting holes on both the

Launchpad circuit board and holes located on the top piece. These holes can be seen in the top piece rendering shown in Figure 21 below.
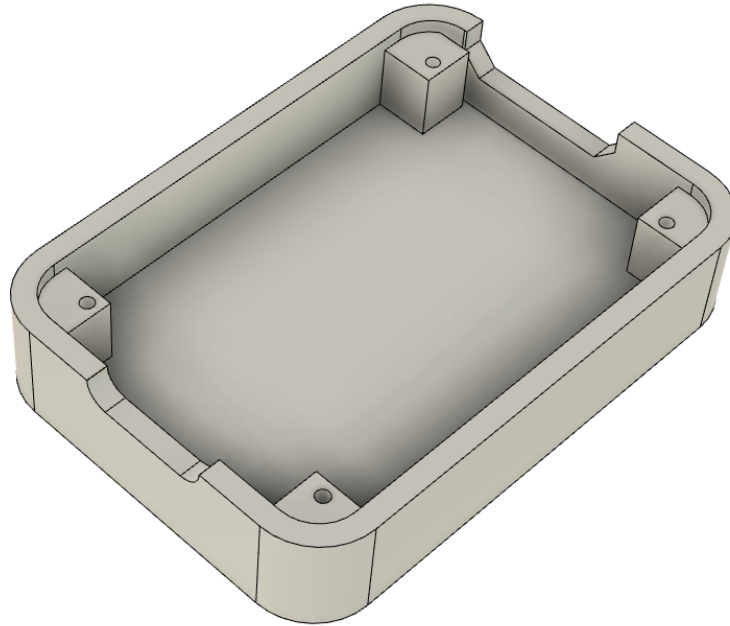

Figure 21. Top Piece of Launchpad Enclosure

Once these two pieces are fitted together in a sort of sandwich fashion, with the PCB in the middle, openings for the micro USB port on the front and 90-degree header pins on the back allow for insertion of the connection cables. A frontal view of this completed assembly is shown below.
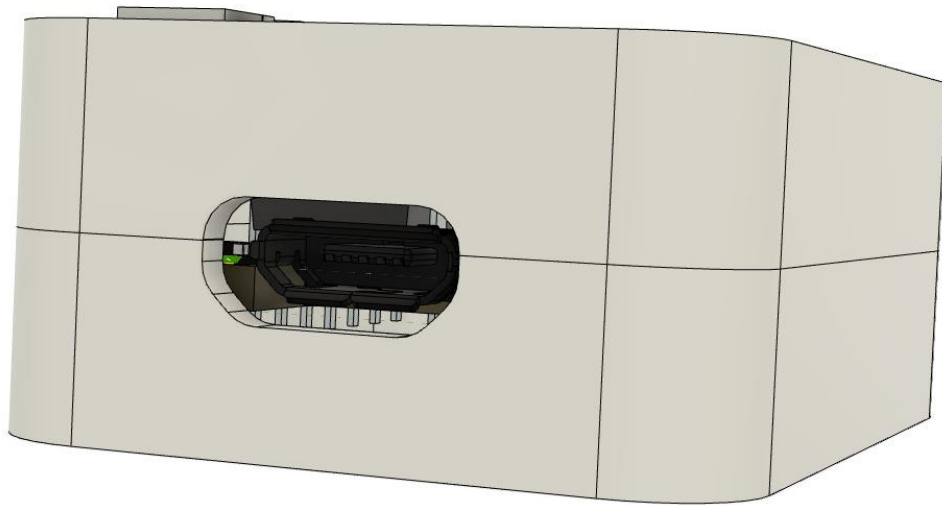
Figure 22. Complete Assembly of Launchpad Enclosure

This simple enclosure was designed to be 3D printed but could also be injection molded in a mass production environment.

To protect against non-ideal conditions, additional circuitry for battery protection and power filtering was also included in this design. The TI LM74700-Q1 is a diode controller chip that uses an external MOSFET to turn off the supply current if an instance of reverse current flow is detected. This feature prevents damage to the motor controller in cases of improper connection to the power supply. This particular chip is designed for use in automotive battery systems as high as 48V and is operable in an ambient temperature environment up to 125 ℃. In addition to the diode controller, a ferrite bead

and decoupling capacitors for extra filtering of the input power are included in this circuitry.

An on-board temperature sensor was included in this design so external equipment was not necessary for testing the thermal characteristics of the device. The component chosen for this function was the TI LMT86QDCKRQ1. This chip meets temperature requirements with an ability to operate in temperatures up to 150 ℃. It also works well under the supply limitations that restrict the microcontroller and all connecting components to an input current less than 70mA. The lower power consumption needs of this chip allow for a voltage supply as low as 2.2V and a current supply as low as 5.4 microamps. This chip also delivers acceptable accuracy of plus/minus 2.7 ℃ over the entire temperature range without calibration.

To allow for the operation of the motor controller after initial programming, a port for three external connections of signals was connected to the microcontroller. After speed control software[3] is loaded to the microcontroller, a user can use this port for basic operation of the motor controller without the need for a PC or external programmer. The user has the option to supply one of two signals: analog or PWM. Using the analog connection, the signal input is controlled via adjustment of voltage from an external supply. Similarly, to use the PWM connection a signal input is sent from an external function generator. The final portion of this circuitry is for diagnostics. It includes a fault

---

[3] Additional discussion regarding this code is written in the algorithm development section later in this chapter

indicator light and a connection to send diagnostic codes, describing device or motor fault statuses, externally.

3.2.3 PCB Layout

A library of components was created for each of the core components in addition to the supporting passive components in the design. The footprints for each of these components were sourced from online libraries with some adjustments being made after careful review. This Eagle library file can be reviewed online through the link listed in Appendix B.

The footprints for these components were then laid out on a circuit board with the following design restrictions:

- Four-layer board

- All components were to be placed on the top layer

- The PCB was required to be in the form of a donut shape with an outer diameter of 90mm and an inner diameter of 30 mm

The main board can be divided into three main sections: Power filtering and reverse battery protection, drive circuitry, and microcontroller/ peripheral connections. Power is externally supplied through a screw terminal and an inductor before reaching the reverse battery protection circuit which is composed of a TI LM74700-Q1 diode controller and supporting passive components. This section was placed at the top of the board with the screw terminal connector placed at about the 12 o'clock mark on the circular board. One special case of component placement is of this section are two large

electrolytic capacitors. They are placed horizontally with a 90-degree wire bend to reduce the vertical space taken up by these relatively tall components. They are located so that they do not interfere with any parts with a height greater than 2.5mm

The drive circuitry is composed of the Allegro A4964 motor driver and its external connections to the three-phase inverter and other supporting passive components. Each phase of the three-phase inverter is composed of a high/low MOSFET pair and some passive components. Each of the MOSFET pairs in the drive circuitry is connected to the A4964 pre-driver on one side and a corresponding connection for each phase of the screw terminal on the other. The screw terminal sits at the bottom of the board and serves as the connection port for an external four-wire BLDC motor.

The microcontroller and peripheral device section is located in the upper right quarter of the PCB. Within the microcontroller circuitry section, there are a few subsections including a connected temperature sensor and external connectors. The first of which is the LMT86QDCKRQ1 temperature sensor that is connected to the ST microcontroller. This component is located between the second and third MOSFET pairs to provide an accurate local temperature reading for what is expected to be the hottest part of the board. Two speed control circuits, one for analog and another for PWM, are connected to a 3-pin header connector that allows for external signal input by a user. The other pin in the three-pin header is used to output diagnostic information from the A4964 to the user. This three-pin connector is located on the right side of the board around the three o'clock mark. Finally, there are a couple of connectors to connect the STM8A microcontroller to

external programmers. This is supported through one of two ports: a two-pin header to connect to the Launchpad, and an ERNI cable connector for connection to the ST-Link programmer. These connectors are placed between the one and three o'clock marks.

The traces within each of the previously mentioned sections were treated differently depending on how much current was expected to be running through them. In general, the traces on the board can be divided into two groups: power level traces/polygons and signal level traces. To make many of the higher power connections on the top layer, several polygons were drawn. The connected nets and functions for each of these polygons are summarized in the table below.

Table VII. Description of Top Layer Polygons

Net Name	Function
+24V	Input power from an external power supply
Unfiltered VCC	Power from supply before reverse protection
VCC	Filtered power from an external supply
VDD	Power supplied to microcontroller from VLR pin of A4964
SA	Return path to A4964 from first MOSFET pair
SB	Return path to A4964 from second MOSFET pair
SC	Return path to A4964 from third MOSFET pair
CSP/CSM	Feedback from lower MOSFETs to the current sense resistor
GND	Return path to GND from the current sense resistor

The SA, SB, and SC polygons make up an area as large as possible given the board size constraints. The VCC and CSP/CSM polygons are connected from other layers to selected areas of the top layer to provide necessary connections to components. To transfer power between each of these layers, a network of vias was placed in these selected locations. A 12 mil size is used for the vias and is uniform throughout. Since this size of via was calculated to carry about 1 amp per 12 mil via, 40 vias per polygon were placed to handle currents up to 40 A.

Most signal level traces were manually routed on the bottom of the board in order to maximize the board space to fit the higher power polygons. The remainder of the signal level traces were routed to make other necessary connections on the top layer. The other three layers in this board design have the following composition:

- Layer 2 – Ground Plane

- Layer 3 – VCC Plane

- Bottom – Signal level traces, CSP/CSM polygon on the upper half, and GND polygon on the lower half

The complete layer by layer stack up is included and annotated in Appendix A.

3.2.4 Development (Work with Allegro Development Board)

With the second design, the importance of testing for functions using a development board remained. In this case, Allegro offered a development board specifically for the

A4964 and this board was acquired. In addition to a variety of supporting passive components and connectors, the development board included three main components: a micro USB port for connection to a PC with Allegro's development software, an 8-bit PIC microcontroller, and a socket for the installation of the included A4964 chips. A 24V Hurst DMA0204024B101 was used as the external brushless DC motor in the initial functional testing of the board.

In addition to the hardware, Allegro also provided software specifically for use with the development board. This software package was available for download through the manufacturer's website and allows for the control of the A4964 registers through the use of an on-board microcontroller via a simple GUI program on a Windows based PC. In addition to being able to change a variety of settings through the registers, the GUI also displays real time data gathered from the motor while in operation.

Once the software is downloaded and the USB cable is connected, the GUI automatically opens up on the PC. To run the motor, the user provides the number of pole pairs and the datasheet value for the no load rated speed of the connected motor. After this setup is completed, settings can be updated through the main window of the GUI shown in figure 23 below.
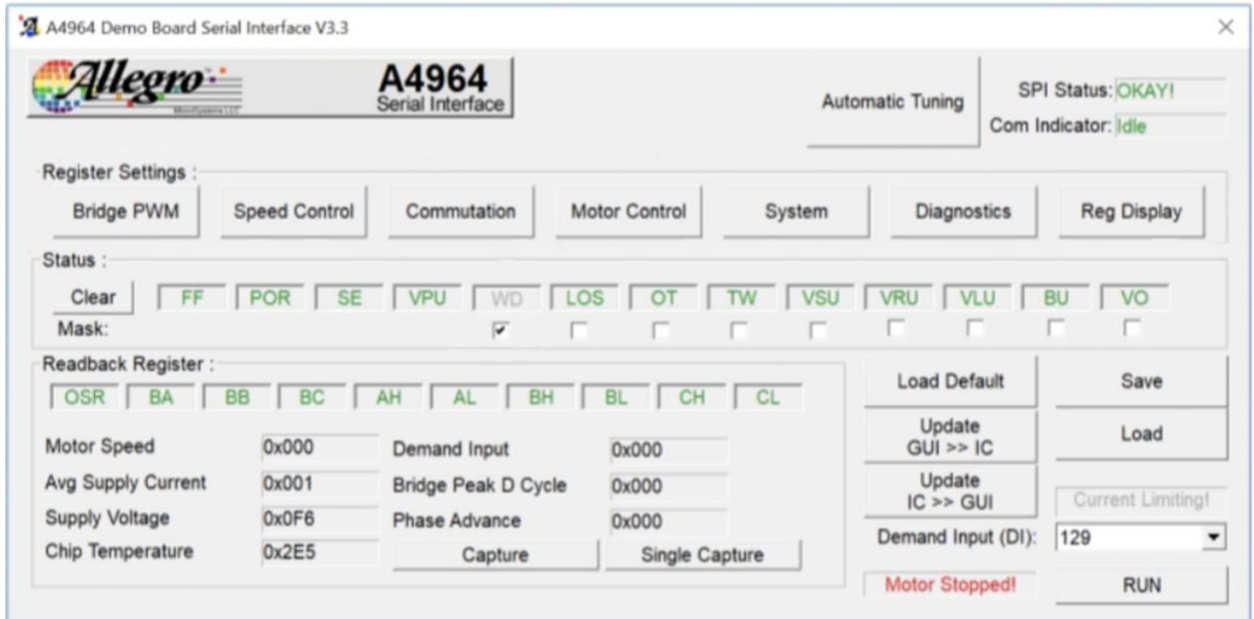
Figure 23. Main Page of the GUI [32]

From here the status register (which contains all the fault information) and the readback

register (which contains physical data points such as the motor speed and chip

temperature) can be seen as the values update in real time. The complete contents of the

A4964 registers can be seen by clicking on the "Register Display" button and the

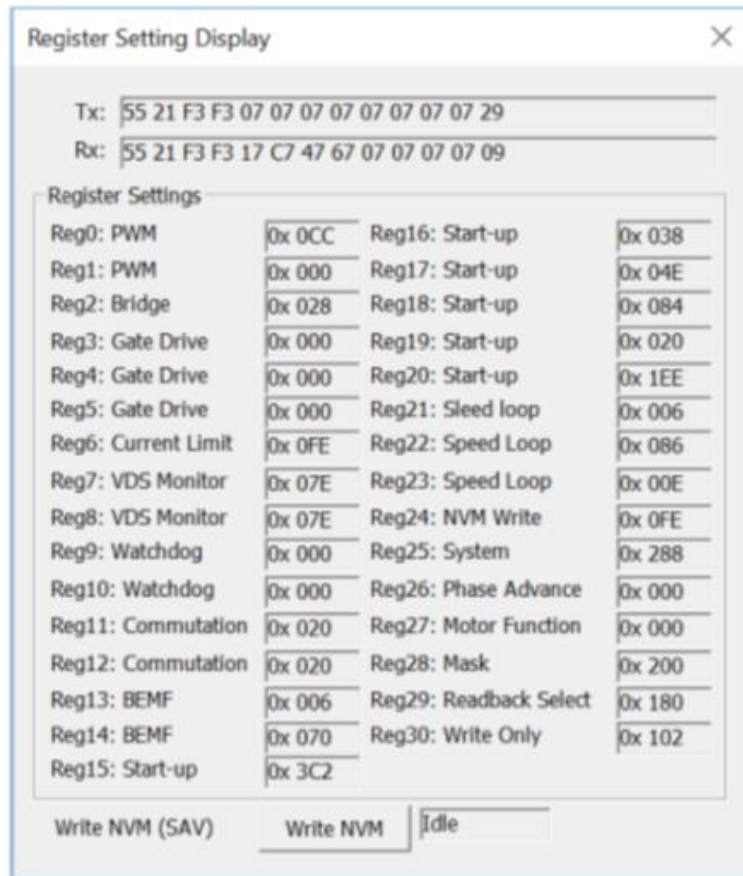resulting screen is shown in figure 24.

Figure 24. Register Contents as shown through the Allegro GUI [32]

As changes to the system's settings are made throughout the GUI, values of the registers

in figure 24 reflect these changes. Once the development board is adjusted such that the

motor is running at desired performance settings, the values of each of the registers can

be copied to an A4964 on a separate prototype board. For example, the drive mode of the

development board can be changed from trapezoidal to sinusoidal by selecting the Bridge

PWM button on the main page and then the sinusoidal drive mode can be selected using a
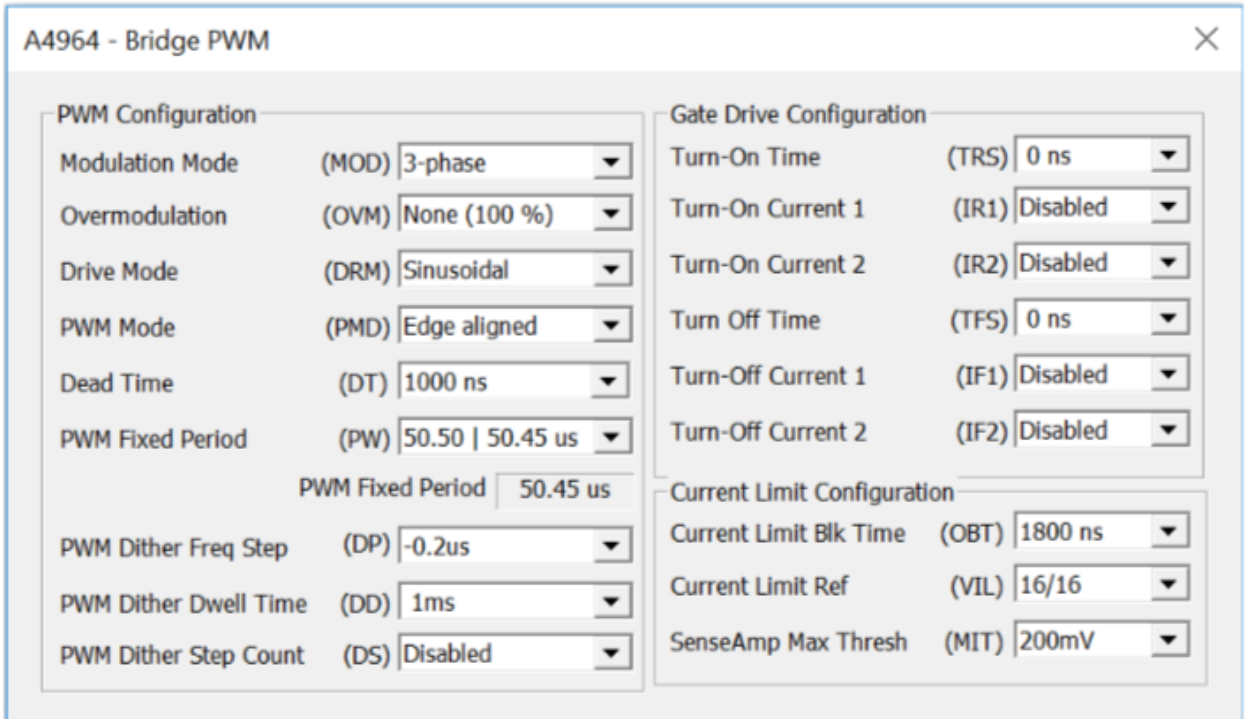
drop-down menu shown in figure 25.

Figure 25. Bridge PWM Settings with Drive Mode Dropdown Menu [32]

After updating the settings via the drop-down menu, the contents of the registers of the A4964 are updated accordingly. A connected motor can then be run using the new settings through the development board or the contents of the register can be copied to the A4964 on the prototype board.

3.2.5 Algorithm Development

To use the additional features designed into the main circuit board such as the user inputs for speed control and the temperature sensor, a program for the microcontroller's function beyond that of simply changing the registers of the A4964 is necessary. The algorithm for this program for running the motor was designed as a state machine. A table of variables for the state machine is shown in the table below.

Table VIII. Summary of Variables Included in the Speed Control Algorithm

Variable Name	Variable Description	Range of Values
Va	The input voltage given by the analog control signal	0-10V uint8_t
PW	The duty cycle given by the PWM signal	0-100% uint8_t
Speed	The speed of the motor expressed as a percentage of maximum speed resulting from maximum input voltage	0-100% uint8_t
Temp	The temperature in Celsius given by the temperature sensor	0-125 °C uint8_t
Run	On/off variable that determines whether the motor is allowed to run based on diagnostic input	Boolean bool
Time_Delay	A timer that allows signal to be sent to the motor before the return to State 0	0-10 ms uint8_t

The state machine can be divided into three main sections titled: Check Input Signals, Thermal Derating, and Output Speed to Motor. The three sections are shown divided into sections for clearer presentation but function in a cohesive flow from one section to the next. The first section for checking input signals to the system is shown below.

Check Input Signals

State 0
Read Input Pins

Analog Pin On
(default)

PWM Pin On
(interrupt detected)

State 1
Read Voltage (Va)

State 2
Read Duty Cycle (PW)

Va<2

PW<15

15<PW<90

2<Va<9.7

State 3
Set Speed to 0%

State 6
Set Speed to 0%

Va>9.7

PW>90

State 5
Set Speed to
25+75/7.7(Va-2)

State 8
Set Speed to
PW+10

State 4
Set Speed to 100%

State 7
Set Speed to 100%

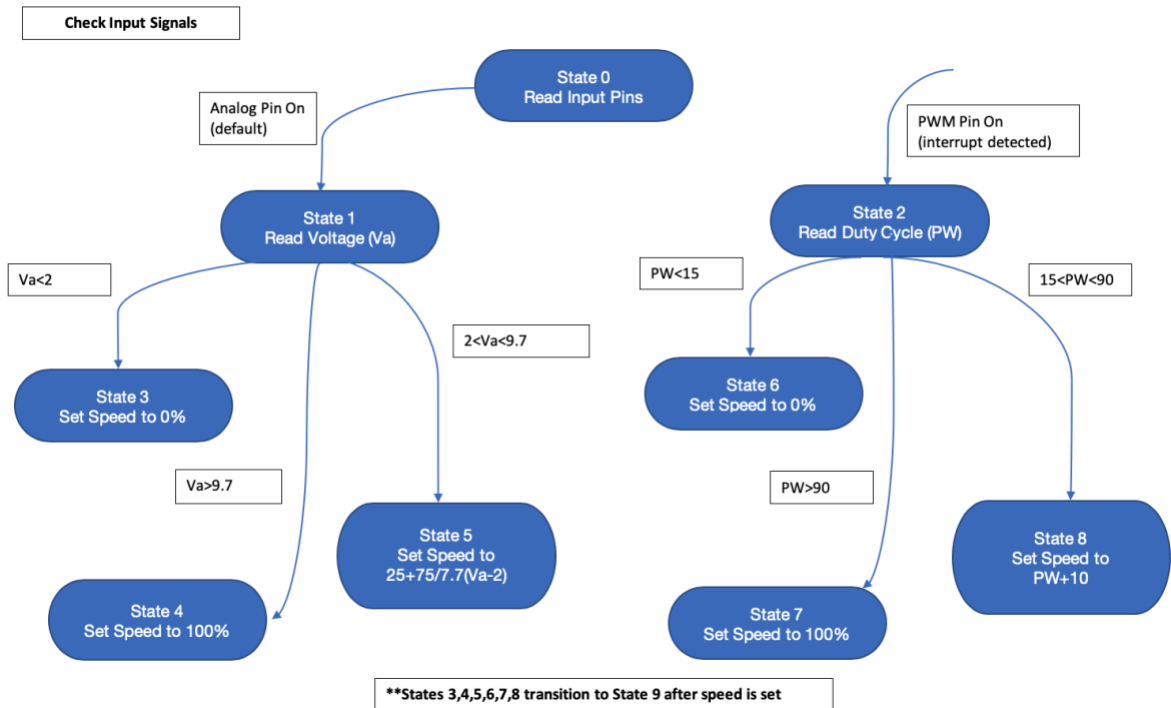**States 3,4,5,6,7,8 transition to State 9 after speed is set

Figure 26. State Machine Diagram Section 1 - Input Signals

In this section, the algorithm checks for an input signal and determines whether the signal is analog or PWM. If a signal is received in state 0 it is assumed to be analog and proceeds to state 1 unless an interrupt, which is designated to search for a PWM signal, is detected. In this case, the algorithm begins in state 2. On each of the two paths a value is given to the signal, read, and stored as a variable. A voltage signal is stored as variable "Va" with units of volts and represents the voltage level received. If a PWM signal is read, the value of the duty cycle is stored as the variable "PW" with duty cycle as the

unit. Based on the reading for each of these signals, the input value of either "Va" or

"PW" is converted into an output value represented by the variable "Speed". For an

analog signal, a voltage of less than 2V is converted to a "Speed" value of zero while a

voltage greater than 9.7 V is converted to a "Speed" value of 100. Any analog signal

between the values of 2V and 9.7V is converted to "Speed" using the following equation

with "Va" as the input value and "Speed" as the output value.

$$Speed = 25 + \frac{(100 - 25)}{(9.7 - 2)}(V_A - 2)$$

For a PWM signal with a "PW" value of less than 15, the resulting "Speed" value is zero.

For a signal with a "PW" value greater than 90, the resulting "Speed" value is 100. For

any "PW" value between 15 and 90 the input value is converted to the output value of

"Speed" using the following equation.

$$Speed = PW + 10$$

After an initial value for "Speed" is determined, the algorithm moves to the thermal

derating section where the "Speed" value is reduced in cases of increased temperature.

This adjustment procedure allows for the motor demand (the ultimate result of the

"Speed" variable) to decrease and avoid the overheating of the controller system. The

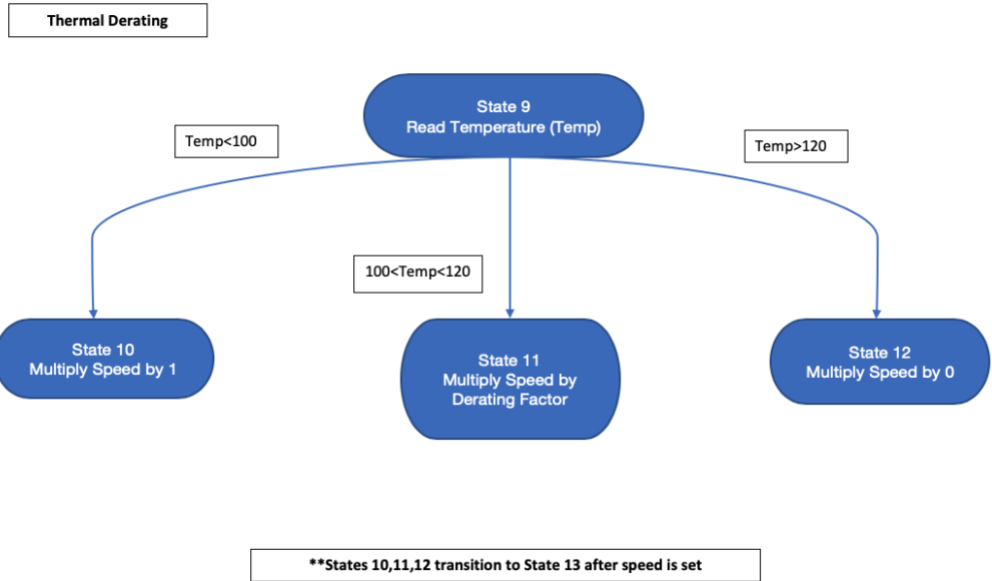thermal derating portion of the state machine diagram is shown below.

Figure 27. State Machine Diagram Section 2 - Thermal Derating

In this section, a value is read from the temperature sensor and the resulting value is stored as the variable name "Temp". For a value under 100, "Speed" is unchanged while a value over 120 results in a "Speed" value of 0. Any value between 100 and 120 is changed by multiplying speed by a derating factor and then stored as the new value of "Speed". This final value of "Speed" is what is sent to the motor after a diagnostic check, detailed in the final segment of the state machine diagram shown in figure 28 below.
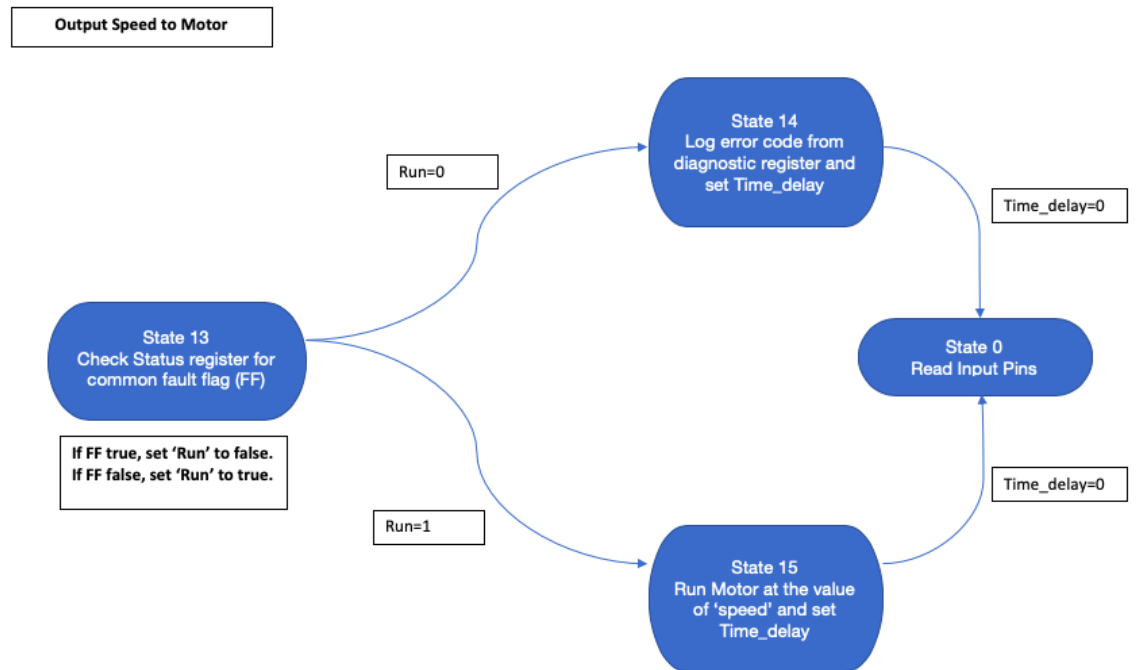
63

Figure 28. State Machine Diagram Section 3 - Speed Output to Motor

Here, the diagnostic register of the A4964 is checked for a common fault flag which is set

if any faults are detected. If this common fault flag is not set, the "Run" variable is set to

1 and the microcontroller sends a command for the motor to run at the currently stored

value of "Speed". If the common fault flag is set, "Run" is set to 0 and the

microcontroller logs the error code from the diagnostic register of the A4964. After each

of these states (14 and 15), a timer is set, and the program returns to State 0 to complete

the algorithm.

This algorithm was created based off of the requirements from an external requirements

document. Implementation of this algorithm into the C code written for the

microcontroller was completed by Ryan Myers as part of his senior project. In the final

software some states were combined but the structure laid out in the state machine

diagram previously described remains valid and is simple to understand.

FABRICATION AND TESTING

Due to the COVID-19 pandemic and the resulting campus closure, facilities and equipment necessary for the fabrication and testing of the completed BLDC controller were not accessible. Since the circuit board could not be completed, a summary of the planned work necessary for completion is listed in this section.

4.1 Planned Fabrication

Upon the receipt of the custom boards and all of the electronic components, each of the boards were planned to be soldered by hand. A custom stencil would be ordered for the main board. An example of a typical stencil for a printed circuit board is shown in the figure below.
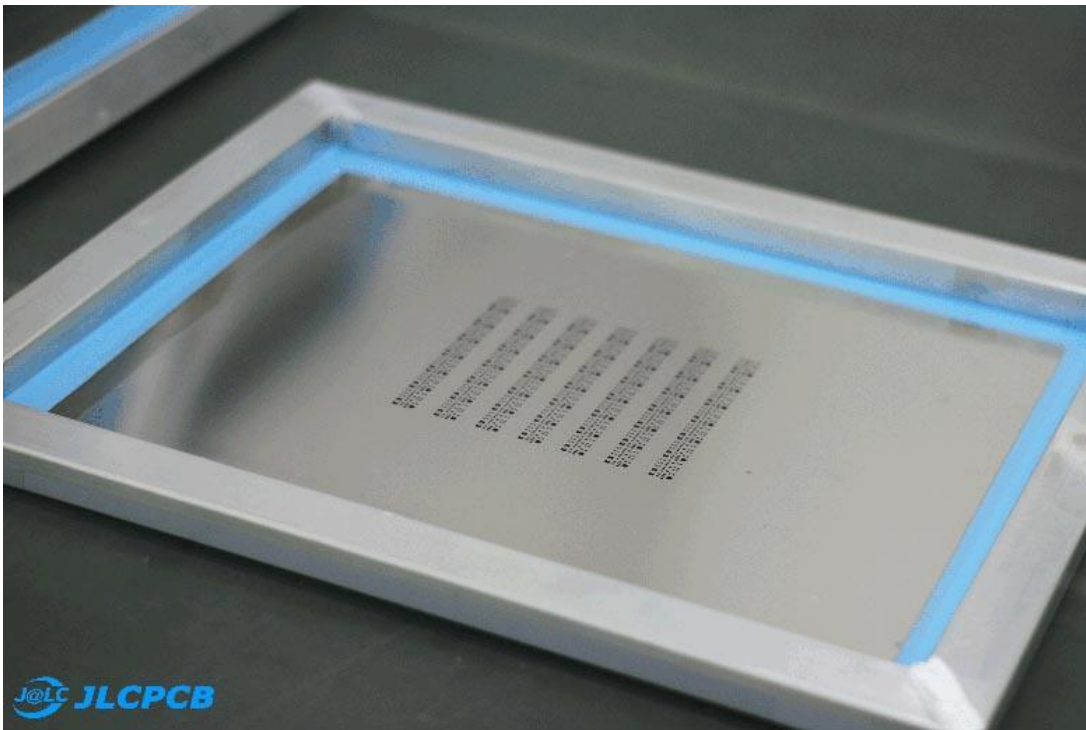

Figure 29. Example of Stencil for Soldering of Surface Mount Components [33]

Using the stencil, solder paste would be applied to the board and surface mount
components would be carefully placed. A rendering of the custom board without
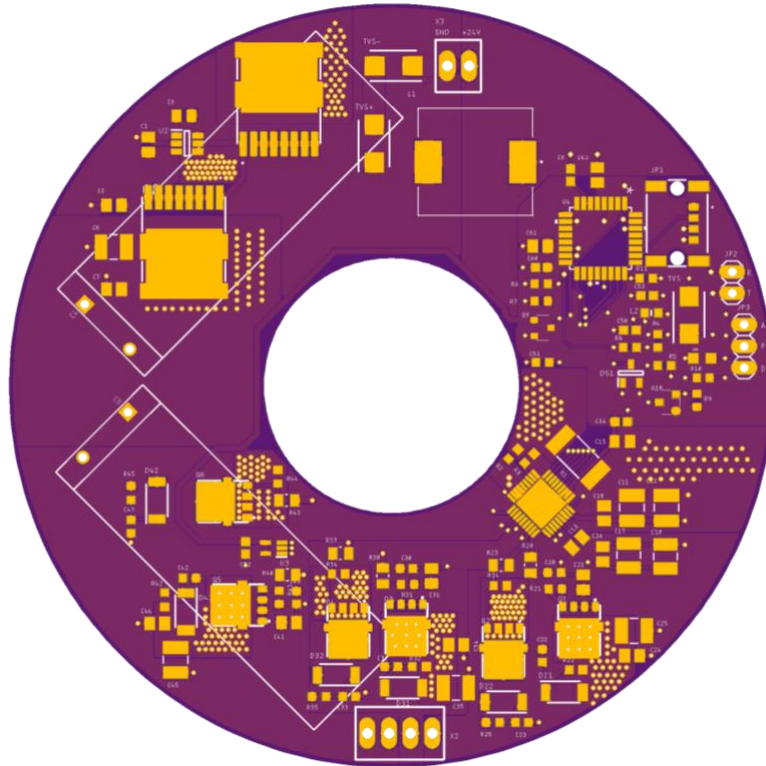components is shown below.

Figure 30. Rendering of Main Circuit Board

After all components were placed, the board would be placed in a reflow oven to flow the
solder. After cooling, final through-hole components would then be soldered by hand
using a soldering iron as would all the components on the Launchpad board.

The enclosure for the Launchpad would be created by exporting the CAD model to an .stl
file and 3D printing it using one of the on-campus printers. The resulting top and bottom

pieces would then be fitted with the completed Launchpad circuit board. A simulated
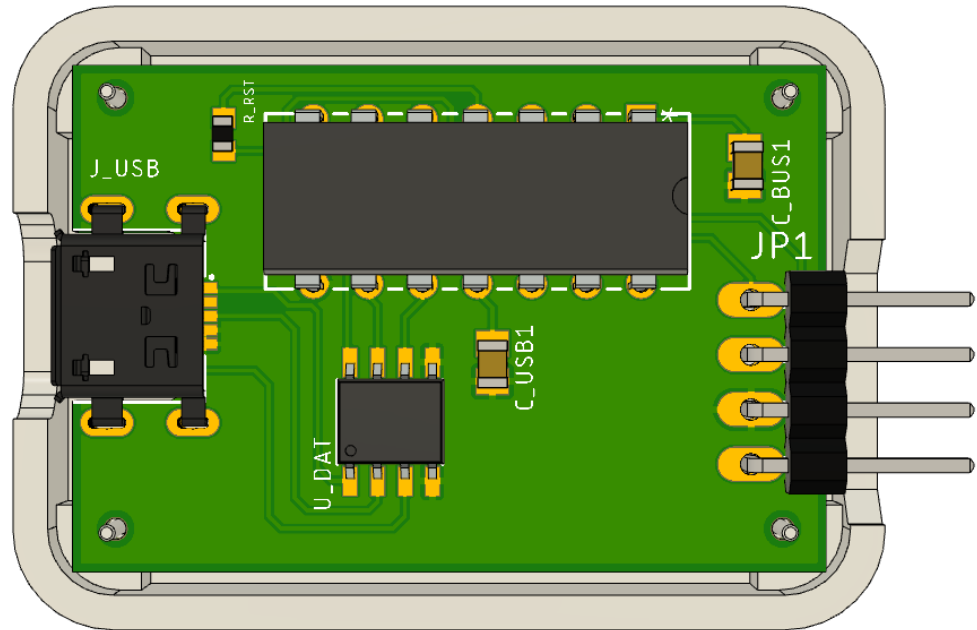
rendering is shown in the figure below.

Figure 31. Rendering of Completed PCB Inserted into Bottom Piece of Enclosure

4.2 Planned Testing

After the fabrication of both the main and Launchpad circuit boards, several functional

tests would be carried out including:

- Connecting the Main Board to an external power supply at 24V

- Connecting the ST-Link to the Main Board via the ERNI connector and included

  cable for programming

- Connecting the Launchpad to a PC and the Main board to test the alternative

  programming method

- Loading the registers of the A4964 on the main board with the desired values from successful development board testing

- Attempting to run the Hurst BLDC motor in the lab with the values exported from the registers of the A4964 on the development board

- Loading the code from the speed control algorithm onto the microcontroller using both the ST-Link and Launchpad programmers

  o Testing the speed control code using the PWM input from an external function generator

  o Testing the speed control code using the Analog input method from an external voltage source

  o Artificially creating a fault state and testing for a diagnostic condition readback

- Operating the system at an incrementally increasing supply current until reaching the objective current of 40 A of input current while documenting the temperature increase and motor output characteristics at each increment

CONCLUSIONS

The original objective for this project was to design and fabricate a printed circuit board based motor control system to drive a three-phase brushless DC motor using a current sensing, sensorless feedback method through the use of automotive grade electronic components. Through the work in this project, a design for a basic BLDC motor controller with a microcontroller-based design was attempted but development was stalled after experiencing technical issues with the design approach. This design was then abandoned for a more favorable route. This updated design was centered around the discovery of a programmable pre-driver solution that is preloaded with firmware to perform various modes of motor operation depending on the settings of its internal registers. A library of footprints for supporting components to the pre-driver was created and laid out into a four-layer printed circuit board design. In addition to this main board, an auxiliary board named Launchpad was created for programming. In order to avoid the use of an exposed board, a simple enclosure was modeled to be fitted with the Launchpad PCB. In addition to the hardware design, an algorithm was drawn up for the standard operation of the main circuit board. The C code written to operate the motor controller was completed by Ryan Myers as part of his senior project. Ultimately, COVID-19 related restrictions prevented the completion of this project but a summary of planned work for the fabrication and testing of the BLDC controller was written.

A summary of future work to be completed includes:

- Ordering the electrical components for the main and Launchpad PCBs

- Ordering the custom PCBs for the main and Launchpad boards

- Ordering a custom stencil for surface mount components for the main board

- Soldering components to the custom main and Launchpad PCBs

- Fabricating and fitting the Launchpad enclosure to the completed Launchpad PCB

- Completion of hardware tests as detailed in Chapter 4

- Programming the speed control C code to the microcontroller on the completed main board

- Completion of software testing and overall system testing as described in Chapter 4

As a result of the inherent complexity and general nature of the design and production of printed circuit boards, it is unlikely that the first prototype produced will be fully functional. It is expected that after some initial testing, errors or shortcomings will become evident. At which point, the design would need to be revised before further testing and overall validation of the system could be completed.

REFERENCES

[1] J. Mouton, "Brushed DC Motor Basics," 2006. [Online]. Available: https://www.microchip.com/stellent/groups/SiteComm_sg/documents/DeviceDoc/en543041.pdf.

[2] S. Ratelet, "Brushless Motors," 2010. [Online]. Available: https://stephane.ratelet.fr/brushless-motors/.

[3] A. Hughes and B. Drury, *Electric Motors and Drives*. 2013.

[4] D. Hanselman, *Brushless Permanent Magnet Motor Design Second Edition*. 2006.

[5] Ravi, "Introduction to Brushless DC Motors," 2019. [Online]. Available: https://www.electronicshub.org/brushless-dc-motor-bldc-motor/.

[6] C. L. Xia, *Permanent Magnet Brushless DC Motor Drives and Controls*. 2012.

[7] J. C. Gamazo-Real, E. Vázquez-Sánchez, and J. Gómez-Gil, "Position and speed control of brushless dc motors using sensorless techniques and application trends," *Sensors*. 2010.

[8] J. Zhao and Y. Yangwei, "Brushless DC Motor Fundamentals," 2011.

[9] S. Uppuluri, "Selecting the Right MOSFETs for Motor Drive Applications," 2016.

[10] K. N. Mogensen, "Motor-control considerations for electronic speed control in drones," *Analog Appl. J.*, pp. 1–7, 2016.

[11] YoungRC, "Brushless Motor ESC," 2020. [Online]. Available: https://www.amazon.com/YoungRC-Brushless-Controller-Multicopter-Quadcopter/dp/B075ZSDR2T?ref_=fsclp_pl_dp_5.

[12] A. M. Harrington and C. Kroninger, "Characterization of Small DC Brushed and Brushless Motors," *Arl-Tr-6389*, 2013.

[13] P. Pickering, "Sine of the Times for BLDC Motors," 2018. [Online]. Available: https://www.electronicdesign.com/automotive/sine-times-bldc-motors.

[14] Zilog, "Zilog Motor Control Technologies: PB025504-0516 [datasheet]," 2016.

[15] Y. L. Karnavas, A. S. Topalidis, and M. Drakaki, "Development of a low cost brushless DC motor sensorless controller using dsPIC30F4011," in *2018 7th International Conference on Modern Circuits and Systems Technologies, MOCAST 2018*, 2018.

[16] K. Kroics, J. Zakis, and U. Sirmelis, "Implementation of the back EMF zero crossing detection for BLDC motor," in *58th Annual International Scientific Conference on Power and Electrical Engineering of Riga Technical University, RTUCON 2017 - Proceedings*, 2017.

[17] W. Brown, "Brushless DC Motor Control Made Easy," 2002. [Online]. Available: http://ww1.microchip.com/downloads/en/appnotes/00857a.pdf.

[18] Renesas Electronics, "BLDC Motor Control Algorithms." [Online]. Available: https://www.renesas.com/in/en/solutions/key-technology/motor-control/motor-

algorithms/bldc.html#.
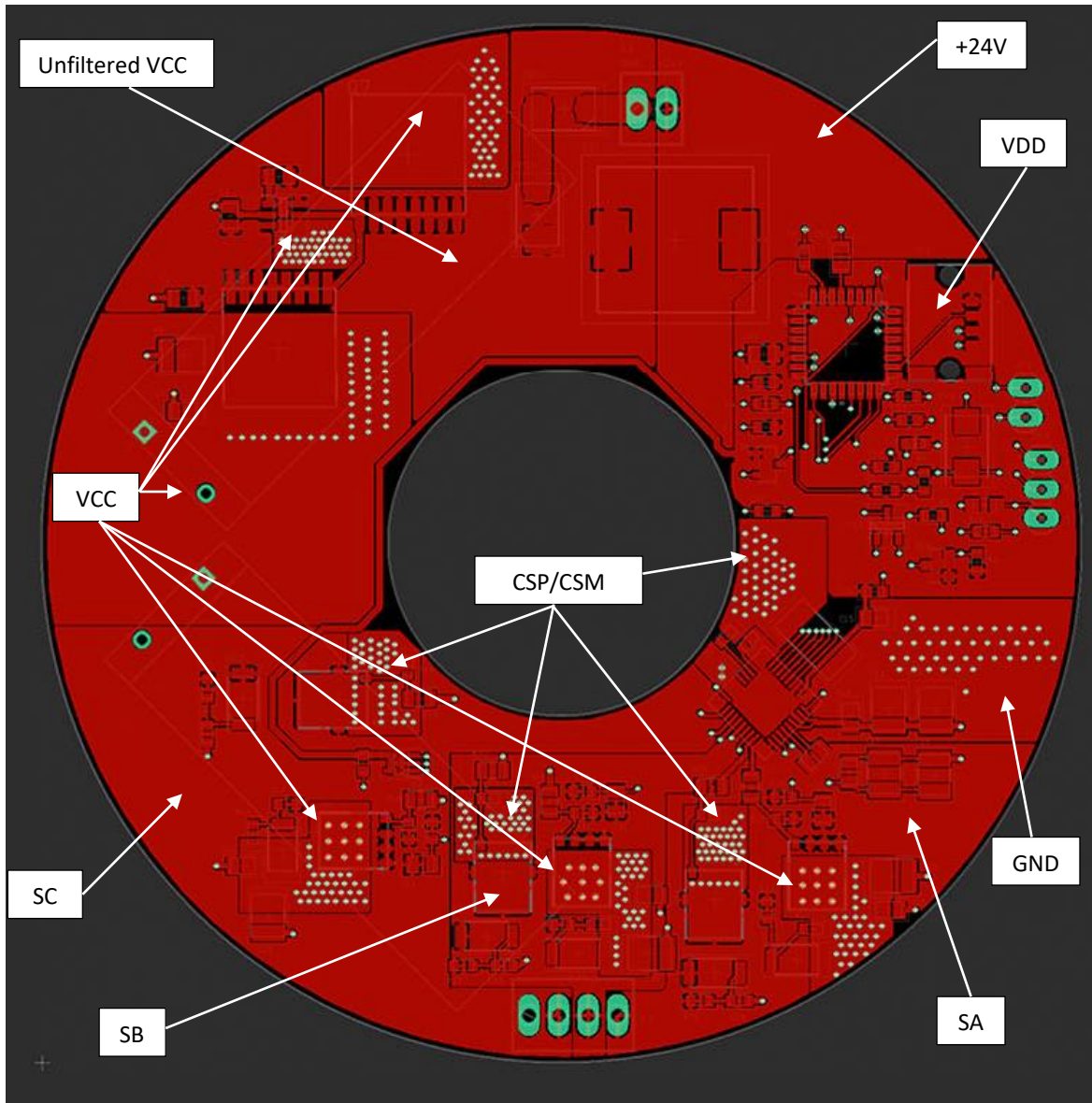
[19] Texas Instruments, "DRV10983-Q1 Automotive, Three-Phase, Sensorless BLDC Motor Driver," 2017. [Online]. Available: https://www.ti.com/lit/ds/symlink/drv10983-q1.pdf.

[20] Digi-Key's North American Editors, "Why and How to Sinusoidally Control Three-Phase Brushless DC Motors," 2017. [Online]. Available: https://www.digikey.com/en/articles/techzone/2017/jan/why-and-how-to-sinusoidally-control-three-phase-brushless-dc-motors.

[21] E. Viramontes, "Motor Control with Freescale Microcontrollers," 2010.

[22] NIT Calicut, "MOSFETs," 2020. [Online]. Available: http://www.rignitc.com/mosfets/.

[23] T. Williams, *The Circuit Designer's Companion*. 2005.

[24] S. Xu and X. Li, "Analysis on thermal reliability of key electronic components on PCB board," in *ICQR2MSE 2011 - Proceedings of 2011 International Conference on Quality, Reliability, Risk, Maintenance, and Safety Engineering*, 2011.

[25] G. Langer, M. Leitgeb, J. Nicolics, M. Unger, H. Hoschopf, and F. P. Wenzl, "Advanced Thermal Management Solutions on PCBs for High Power Applications," 2020. [Online]. Available: http://www.ipc.org/feature-article.aspx?aid=Advanced-Thermal-Management-Solutions-on-PCBs-for-High-Power-Applications.

[26] Y. Shen, H. Wang, F. Blaabjerg, H. Zhao, and T. Long, "Thermal modeling and design optimization of PCB vias and pads," *IEEE Trans. Power Electron.*, 2020.

[27] T. A. Asghari, "PCB thermal via optimization using design of experiments," in *Thermomechanical Phenomena in Electronic Systems -Proceedings of the Intersociety Conference*, 2006.

[28] Automotive Electronics Council, "AEC-Q100 - Failure Mechanism Based Stress Test Qualification for Integrated Circuits," *AEC - Q100 Rev-H*, 2014. [Online]. Available: http://www.aecouncil.com/Documents/AEC_Q100_Rev_H_Base_Document.pdf.

[29] Automotive Electronics Council, "Aec-Q200 - Stress Test Qualification for Passive Components," 2010. [Online]. Available: http://www.aecouncil.com/Documents/AEC_Q200_Rev_D_Base_Document.pdf.

[30] J. De Viaene, F. Verbelen, S. Derammelaere, and K. Stockman, "Energy-efficient sensorless load angle control of a BLDC motor using sinusoidal currents," *IET Electr. Power Appl.*, 2018.

[31] P. S. Chaudhari, S. L. Patil, S. K. Pandey, and S. Sinha, "Performance analysis of BLDC motor on sinusoidal and square wave supply," in *IEEE International Conference on Power Electronics, Drives and Energy Systems, PEDES 2016*, 2017.

[32] Allegro MicroSystems LLC, "Sensorless, Sinusoidal Drive BLDC Controller,"

2018. [Online]. Available: https://registration.allegromicro.com/#/parts/A4964K.

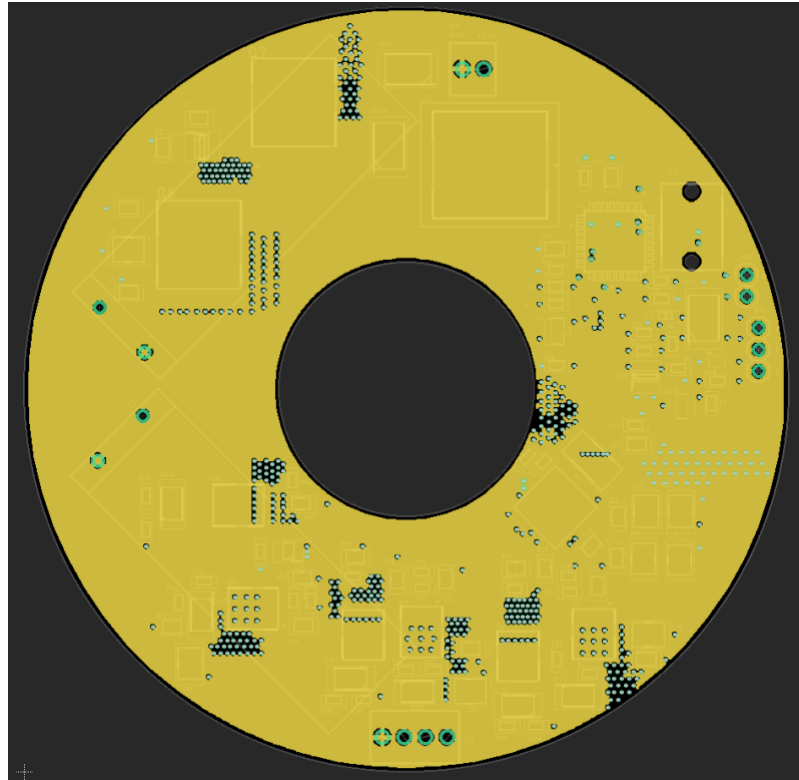[33] bangmuin.xyz, "Smd Stencil Framework," 2020. [Online]. Available: http://bangmuin.xyz/smd-stencil-framework/.

A. Layer by Layer Annotated Images of the Final Routing

Top Layer

Layer 2 – Ground Plane

Layer 3 – VCC Plane

Bottom Layer

Ground Polygon
(unfilled for clarity)

CSP/CSM Polygon
(unfilled for clarity)
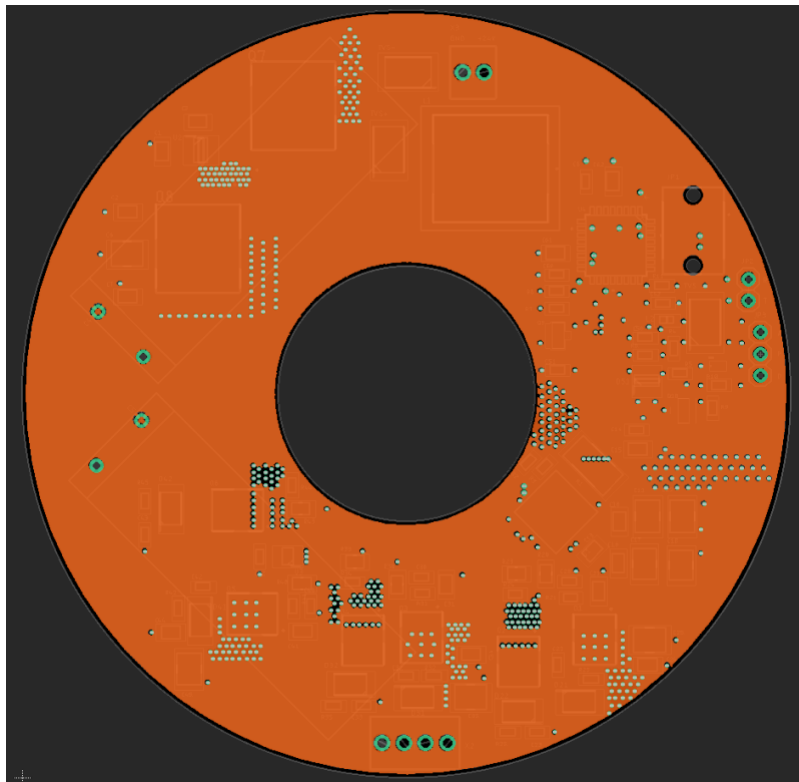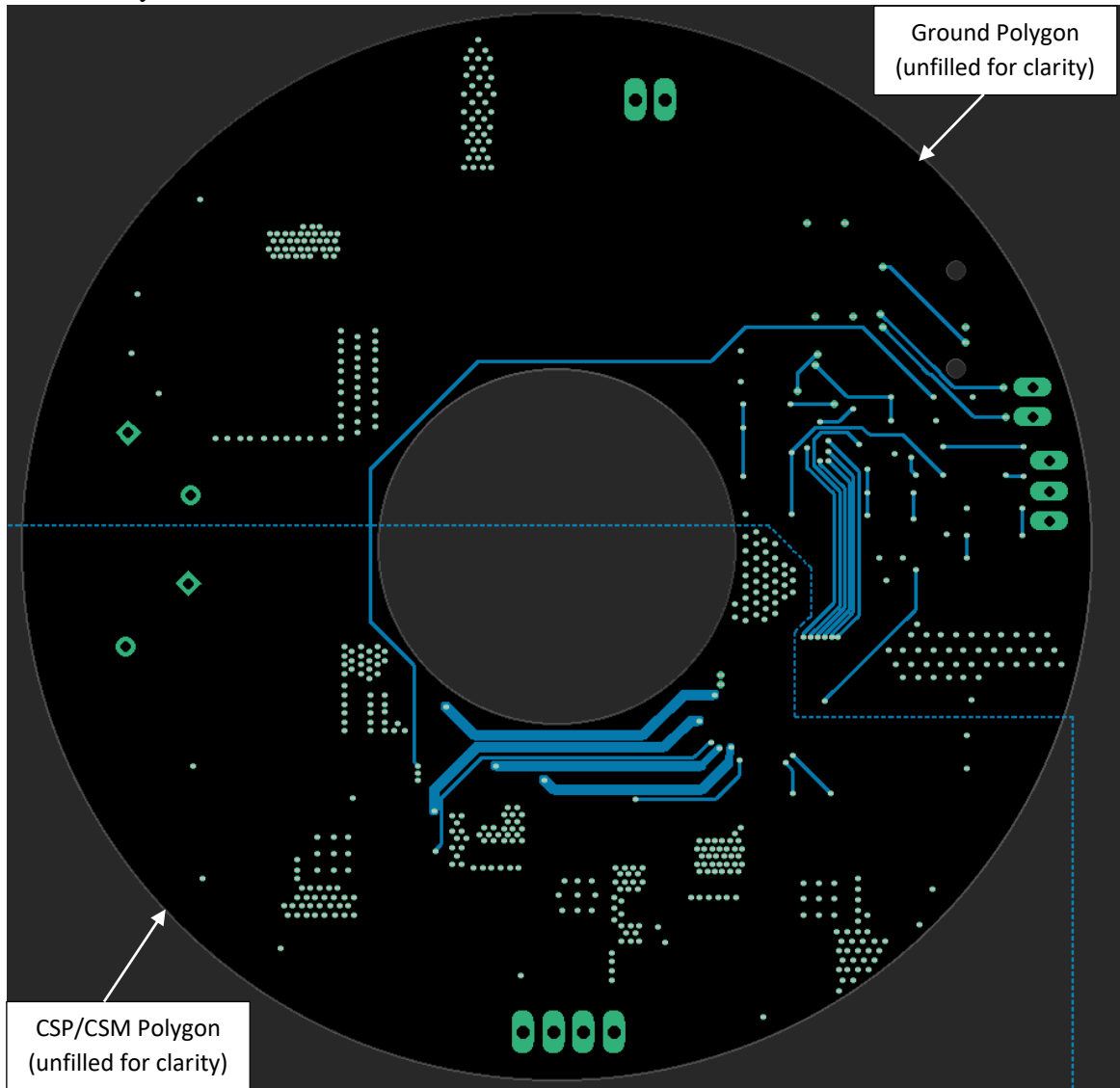
B. Online Reference Files

Files for the Autodesk Eagle board design and corresponding Eagle part library files are available along with .stp Launchpad enclosure files through the web address listed below.

https://github.com/jtcastle/BLDC-Motor-Controller